Current Research in Toxicology 6 (2024) 100169

Contents lists available at ScienceDirect

Current Research in Toxicology

journal homepage: www.journals.elsevier.com/current-research-in-toxicology

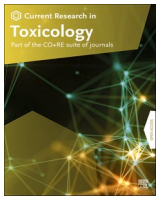

Research Paper

Comparing the effects of three neonicotinoids on embryogenesis of the South African clawed frog *Xenopus laevis*

Hannah Flach [1], Carla Brendler [1], Martina Schöpf, Lilly Xu, Julia Schneider, Kathrin Dewald, Petra Dietmann, Michael Kühl, Susanne J. Kühl [*]

Institute of Biochemistry and Molecular Biology, Ulm University, Albert-Einstein-Allee 11, 89081 Ulm, German

ARTICLE INFO

Keywords:
Embryogenesis
Neonicotinoids
Pesticides
Xenopus laevis
Insecticides

ABSTRACT

Neonicotinoids (NEOs) are widely used insecticides that are ubiquitous in agricultural use. Since NEOs are found in natural waters as well as in tap water and human urine in regions where NEOs are widely used, NEOs pose a potential hazard to non-target organisms such as animals and humans. Some of the commonly detected NEOs are imidacloprid (IMD), thiamethoxam (TMX), and its metabolite clothianidin (CLO). Although previously published scientific information, including an assessment of the environmental risks, particularly for bees, had resulted in a ban on the outdoor use of these three NEOs in the EU – their use is now only permitted in closed greenhouses – these NEOs continue to be used in agriculture in many other parts of the world. Therefore, a detailed study and comparison of the effects of NEOs on the embryonic development of non-target organisms is needed to further define the risk profiles.

Embryos of the South African clawed frog *Xenopus laevis*, a well-established aquatic model, were exposed to different concentrations of IMD, TMX, or CLO (0.1–100 mg/L) to study and compare the possible effects of a single contaminant in natural water bodies on early embryogenesis. The results included a reduced body length, a smaller orbital space, impaired cranial cartilage and nerves, and an altered heart structure and function. At the molecular level, NEO exposure partially resulted in an altered expression of tissue-specific factors, which are involved in eye, cranial placode, and heart development.

Our results suggest that the NEOs studied negatively affect the embryonic development of the non-target organism *X. laevis*. Since pesticides, especially NEOs, pollute the environment worldwide, it is suggested that they are strictly controlled and monitored in the areas where they are used. In addition, the question arises as to whether pesticide metabolites also pose a risk to the environment and need to be investigated further so that they can be taken into account when registering ingredients.

Introduction

The use of pesticides continues to increase worldwide (FAO, 2023). Their use is often prophylactic, with many farmers trying to protect their crops from potentially harmful weeds, fungi, and insects (Lechenet et al., 2017). One well-known group of insecticides is the neonicotinoids (NEOs). These synthetic, nicotine-like chemicals reliably control insects by binding and activating the nicotinic acetylcholine receptor (nAChR) (Ihara and Matsuda, 2018; Matsuda et al., 2001). The first NEO, imidacloprid (IMD), was introduced in 1991 (Kagabu, 2011). Many others followed, including thiamethoxam (TMX) in 1998 and its metabolite clothianidin (CLO) in 2002 (Schäfer, 2008). The selectivity of NEOs was anticipated to be only for insects, with this efficacy offering decisive pest control advantages (Ihara and Matsuda, 2018; Tomizawa and Casida, 2003). As a result, NEOs became one of the leading insecticide classes in the global market (Douglas and Tooker, 2015; Jeschke et al., 2011).

In recent years, however, there have been increasing concerns about their safety and impact on non-target organisms. Due to the threat NEOs pose to honeybees, the use of the NEOs IMD, TMX and CLO in the EU was limited in 2018 to permanently existing greenhouses (European Commission, 2018). It is, however, possible to obtain time-limited permits for specific NEO uses within the EU. For example, TMX was granted special approval for use in sugar beet pickling in Germany from 2020 to 2021 and more recently in England in 2022 (Bundesamt für

* Corresponding author at: Institute of Biochemistry and Molecular Biology Ulm University, Albert-Einstein-Allee 11, 89081 Ulm, Germany.
E-mail address: Susanne.kuehl@uni-ulm.de (S.J. Kühl).
[1] Equal contribution

https://doi.org/10.1016/j.crtox.2024.100169
Received 28 September 2023; Received in revised form 16 April 2024; Accepted 18 April 2024
Available online 21 April 2024

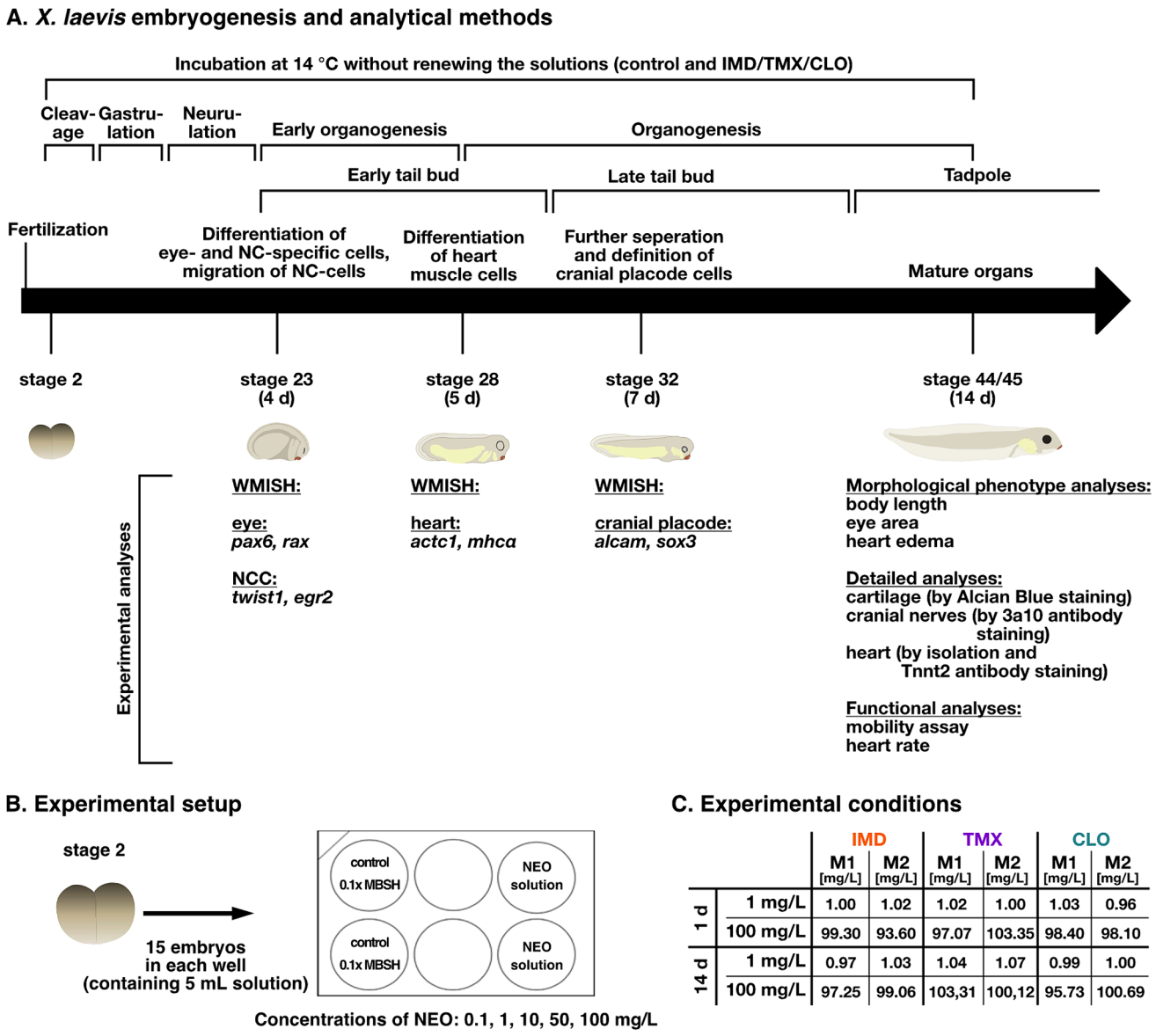

		IMD		TMX		CLO	
		M1 [mg/L]	M2 [mg/L]	M1 [mg/L]	M2 [mg/L]	M1 [mg/L]	M2 [mg/L]
1 d	1 mg/L	1.00	1.02	1.02	1.00	1.03	0.96
	100 mg/L	99.30	93.60	97.07	103.35	98.40	98.10
14 d	1 mg/L	0.97	1.03	1.04	1.07	0.99	1.00
	100 mg/L	97.25	99.06	103,31	100,12	95.73	100.69

Fig. 1. Timeline of *X. laevis* Development and Stability of the Different NEOs. A. *X. laevis* embryogenesis and analytical methods. After the fertilization, the 2-cell-stage embryos were incubated in the control and NEO (IMD/TMX/CLO) solutions until they reached the desired stage. Embryos at stage 23 (four incubations days), stage 28 (five incubation days) and stage 32 (seven incubation days) were used for WMISH staining. For the morphological phenotype as well as the detailed and functional analyses we used stage 44/45 embryos that had been incubated in a NEO solution for 14 days. B. Experimental setup. Two times 15 *X. laevis* embryos at stage 2 were incubated in 5 mL of different NEO solutions (0.1 – 100 mg/L) or 0.1x MBSH (control) at 14 °C. C. Experimental conditions. To determine the exact NEO concentrations on day 1, two sets of 1 and 100 mg/L NEO solutions were sent to an analytical lab. The same solutions were analyzed after 14 days to determine possible changes in concentrations over the incubation time. Abbreviations: NEO, neonicotinoid; IMD, imidacloprid; TMX, thiamethoxam; CLO, clothianidin; M1, measurement 1; M2, measurement 2; d, days; WMISH, whole mount *in situ* hybridization; mL, milliliter; mg/L, milligram per liter.

Verbraucherschutz und Lebensmittelsicherheit, 2022). In other parts of the world (e.g. the United States, Brazil and Asia), NEOs are still registered and widely used without special restrictions (Environmental Fate and Effects Division Office of Pesticide Programs, 2023; Miles et al., 2017; YongFan, 2015). In addition to aerial and ground foliar applications and soil applications, the NEOs IMD, TMX and CLO are currently approved for seed treatment, chemical irrigation and for use in bait. The NEO IMD is also approved for pet collars and crab control (Environmental Fate and Effects Division Office of Pesticide Programs, 2023).

Neonicotinoids are ubiquitous in the global environment. In areas where the use of NEOs is widespread, they may pose a direct threat to humans, since they can be found not only in drinking and tap water (Wan et al., 2020), but also in the urine of the human population in these areas, including children and pregnant women (Mahai et al., 2022; Ikenaka et al., 2019). Neonicotinoids even occur in high concentrations in some areas of the world in natural waters (IMD up to 0.32 mg/L (Netherlands), TMX up to 0.55 mg/L (Mexico), CLO up to 0.17 mg/L (United States)) (Megchún-García et al., 2018; Miles et al., 2017; Van Dijk et al., 2013), bringing a variety of non-target organisms into contact with the NEOs. Therefore, it is of particular interest to understand the risk that the use of certain NEOs poses to aquatic non-target organisms and how NEOs potentially affect their embryonic development and thus their condition and survival. Amphibians are especially threatened by biodiversity loss, with various causes such as habitat loss, climate change, infectious diseases, or contaminants being responsible for the amphibian extinction (Collins, 2010). Pesticide residues can enter natural waters through leaching, run-off, or "worst-case" scenarios (e.g., incorrect handling or improper disposal), which brings amphibians into

contact with the pesticides (Foley et al., 2005). For this reason, it is important to study the possible effects of NEOs on amphibians.

There are few studies about the effects of different NEOs on aquatic vertebrates (Malhotra et al., 2021) showing that the NEOs IMD, TMX and CLO can affect morphological development of various tissues and organs, organ function, and behavior. For example, IMD has been linked to a stress syndrome and associated susceptibilities to ectoparasites in adult Japanese medaka fish (*Oryzias latipes*) (Sánchez-Bayo and Goka, 2005). Imidacloprid induced toxicity and gene expression in zebrafish (*Danio rerio*) embryos (Wu et al., 2018). Exposure of rainbow trout (*Oncorhynchus mykiss*) embryos to TMX resulted in a loss of balance and altered swimming behavior (Finnegan et al., 2017). Clothianidin was shown to reduce responsiveness of adult crayfish (*Orconectes propinquus*) to stimuli, and a negative effect on the feeding behavior of aquatic insects (*Belostoma flumineum*) (Miles et al., 2017). Due to the paucity of data, more studies are needed on the effects of NEOs on various non-target aquatic species to perform more comprehensive risk assessments.

The well-established aquatic model organism *Xenopus laevis,* the South African clawed frog, provides a suitable model for embryological toxicity studies (Flach et al., 2023b, 2023a, 2022; Tandon et al., 2017). Therefore, *X. laevis* was used here to research and compare the effects of the three NEOs IMD, TMX and CLO on early embryonic development. In particular, we analyzed the effect of these three NEOs on embryonic morphology and mobility as well as development of cranial cartilage, cranial nerves and cardiac structure and function including the heart rate. In addition, tissue-specific gene expression was investigated to compare possible effects of the three NEOs at the molecular level. In particular for the investigation of the eye development, we used the transcription factors *pax6* (paired box 6) and *rax* (retina and anterior neural fold homeobox 1), because both are required during eye-cell differentiation (Andreazzoli et al., 2003; Lupo et al., 2000; Ziman et al., 2001). The transcription factors *twist1* (twist family bHLH transcription factor 1) and *egr2* (early growth response 2), both involved in neural crest cell (NCC) induction and migration, were used to investigate the NCC differentiation and migration (Bradley et al., 1993; Hopwood et al., 1989). The adhesion molecule *alcam* (activated leukocyte cell adhesion molecule), that is specifically expressed in the cranial placodes and ganglia, and the transcription factor *sox3* (SRY-box 3), that is expressed and involved in placodal development, were used to investigate cranial placode development (Gessert et al., 2008; Schlosser, 2006; Schlosser and Ahrens, 2004). To investigate myocardial differentiation, the structural proteins *actc1* (actin alpha cardiac muscle 1) and *mhcα* (alpha-myosin heavy chain), both expressed during cardiac development, were used (Garriock et al., 2005; Gessert and Kühl, 2009).

Experimental procedures

The aquatic model organism Xenopus laevis.

The extraction, fertilization and cultivation of *X. laevis* eggs and embryos were performed according to standard protocols (Sive et al., 2000). The female frogs were stimulated to lay eggs with 800 U human chorionic gonadotropin (hCG, HiSS Diagnostics GmbH, Germany) injection and were induced to spawn by gently stroking the abdominal region. A colony of 310 female frogs was used to obtain the eggs during the experimental period of this study. The isolated testes from male frogs were chopped and mixed with 1x MBSH (Modified Barth's saline containing a HEPES buffer [10 mM HEPES ([2-hydroxyethyl]-1-piperazineethanosulforic-acid), 88 mM NaCl, 1 mM KCl, 0.33 mM $Ca(NO_3)_2$ x $(H_2O)_4$, 0.41 mM $CaCl_2$ x $(H_2O)_2$, 0.82 mM $MgSO_4$ x $(H_2O)_7$, 2.4 mM $NaHCO_3$] with pH 7.4) to create a testicular suspension, which was used for fertilization purposes. The testicular suspension of one male frog was used for fertilization over a period of two weeks. A total of 49 male frogs were used during this study. The oocytes from one female were fertilized with a testicular suspension diluted 1:10 with double-distilled H_2O. The fertilized eggs were incubated, and the jelly coats were removed with 2 % L-cysteine (Sigma-Aldrich, Germany) until the embryos reached the 2-cell-stage as described in the NF-stages by Nieuwkoop and Faber (Nieuwkoop and Faber, 1954). All procedures were performed in accordance with the German Animal Protection Act and approved by the local state administration of Baden-Württemberg (*Regierungspräsidium Tübingen*; AZ: 35/9185.82–3).

Exposure of X. laevis embryos to IMD, TMX and CLO

In order to examine the effects of the NEOs IMD, TMX and CLO (Sigma-Aldrich, Germany), fertilized eggs were incubated in single-pesticide-solutions from the 2-cell-stage for a maximum of 14 days (Fig. 1A, B). The pesticide solutions were prepared by dissolving the respective NEO in 0.1x MBSH. Concentrations were 0.1, 1, 10, 50 to 100 mg/L. The exposure of embryos to 0.1 and 1 mg/L of each NEO reflects environmentally relevant concentrations (Megchún-García et al., 2018; Miles et al., 2017; Van Dijk et al., 2013), with 10, 50 and 100 mg/L NEO representing "worst-case" scenarios (e.g., incorrect handling or improper disposal) (Huyen et al., 2020).

For each solution, 15 embryos from one artificial fertilization event (from one female frog) at the 2-cell-stage were transferred into a single well of a 6-well-plate filled with 5 mL solution, in duplicate, thus a total of 30 embryos (n = 30) each from the same fertilization event were incubated (Fig. 1B). The embryos from one artificial fertilization event / from one female frog constituted one embryo batch. In most experiments, several embryo batches were analyzed to account for normal biological variations. The embryos were incubated according to the natural day/night cycle. The same experimental design has been used previously (Flach et al., 2023b, 2023a, 2022; Kerner et al., 2023).

Observations on potential morphological changes (i.e., body length, eye area, heart edema) were made on the embryos incubated in a control solution (0.1x MBSH) or NEO treatment solution. Depending on the biological endpoint, the NEO treatment concentration varied so to perform more detailed analyses (see below).

Analyses of the NEO concentrations and stability

To analyze the NEO concentrations (IMD, TMX and CLO) during the incubation period, we prepared 100 mL of two concentrations (1 and 100 mg/L) of each NEO by diluting IMD, TMX and CLO in 0.1x MBSH. After the dilution, 50 mL of both NEO concentrations (IMD/TMX/CLO) were tested by an independent analytical lab (SGS Analytics GmbH, Germany) on day 1. The other 50 mL of each concentration were incubated for 14 days. We kept the external influences on the solutions identical to the experimental setup described (incubation at 14 °C; natural day/night cycle; 5 mL in each well of a 6-well plate) but did not incubate any embryos to avoid a potential solution contamination caused by dying embryos. After the incubation period of 14 days, 50 mL of each solution was analyzed. Duplicates were performed (Fig. 1C).

Embryonic mobility

To determine possible effects on embryo mobility, the total distance moved by embryos was measured in the control solution (0.1x MBSH), 10 mg/L, and 100 mg/L of each NEO until NF-stage 44/45. The embryos in triplicate (three embryos per embryo batch) were recorded in parallel in 5 mL solution in a petri dish (diameter: 3.2 cm) and with a camera (acA1300-30gc, Basler, Germany (CS-Mount Computer Objective 2.8–12 mm 1:1.3 IR 1/3″, Bangladesh; sample rate: 25 fps; resolution: 1024x768)) (Flach et al., 2023b) for two hours at room temperature (20 ± 1 °C) after equilibration to room temperature (20 ± 1 °C) to avoid temperature fluctuation effects. This approach was repeated three to four times for the same embryo batch. In total, two to three independent embryo batches were analyzed for each NEO concentration. The total distance moved was evaluated with the tracking software Ethovision XT 13 (Noldus, Netherlands). Embryos that the software was unable to

Table 1
Overview over gene probes used in WMISH approaches. These probes have already been used in previous studies to analyze the specified developmental process (examples are given in the right column).

Gene name	Gene function	Genes involved during early development	Examined NF-stage	Gene probes specific for
pax6 (paired box 6)	transcription factor	expressed in and required for eye development (Ziman et al., 2001)	23	eye differentiation (used in e.g. Bugner et al., 2011; Cizelsky et al., 2013; Flach et al., 2021; Gessert et al., 2010; Rothe et al., 2017; Tamanoue et al., 2006)
rax (retina and anterior neural fold homeobox 1)	transcription factor	expressed in and required for eye development (Andreazzoli et al., 2003; Lupo et al., 2000)	23	eye differentiation (used in e.g. Cizelsky et al., 2013; Gessert et al., 2010; Kiem et al., 2017; Rothe et al., 2017; Seigfried et al., 2017; Strate et al., 2009)
twist1 (twist family bHLH transcription factor 1)	transcription factor	expressed in neural crest cell development (Hopwood et al., 1989)	23	neural crest cell migration (used in e.g. Flach et al., 2018; Gessert et al., 2010; Kiem et al., 2017; Wang et al., 2021)
egr2 (early growth response 2)	transcription factor	expressed in and required for neural crest cell development (Bradley et al., 1993)	23	neural crest cell differentiation (used in e.g. Gessert et al., 2010; Kiem et al., 2017; Park and Saint-Jeannet, 2008)
alcam (activated leukocyte cell adhesion molecule)	adhesion molecule	expressed in cranial placode and ganglia development (Gessert et al., 2008)	32	cranial placode development (used in e.g. Saumweber et al., 2024)
sox3 (SRY-box 3)	transcription factor	expressed in and required for cranial placodal development (Schlosser, 2006; Schlosser and Ahrens, 2004)	32	cranial placode development (used in e.g. Saumweber et al., 2024; Schuff et al., 2007)
actc1 (actin alpha cardiac muscle 1)	structural protein	expressed in cardiac development (Gessert and Kühl, 2009)	28	cardiac cell differentiation (used in e.g. Brade et al., 2007; Gessert et al., 2008; Hempel et al., 2017; Peterkin et al., 2007)
mhcα (alpha-myosin heavy chain)	structural protein	expressed in and required for cardiac development (Garriock et al., 2005)	28	cardiac cell differentiation (used in e.g. Gentsch et al., 2018; Gessert et al., 2008; Gessert and Kühl, 2009; Guo et al., 2019; Hempel et al., 2017)

detect for more than 10 % of the recording time were not included in the statistical evaluations ending in n = 19–27 single analyzed embryos per experimental approach.

Heart rate measurements

Embryos in the control and the NEO solutions (1, 10, 50, 100 mg/L each) were incubated up to stage 44/45 (see Section "Exposure of *X. laevis* embryos to IMD, TMX and CLO"; Fig. 1A, B). The heartbeats of ten individual embryos (n = 10) of three independent embryo batches were documented for one minute at room temperature (20 ± 1 °C). In particular, one embryo was put into one well of a 6-well plate containing 5 mL 0.1x MBSH. Under a light microscope (Olympus SZH10 and SZX12, Olympus, Germany) the heartbeat was observed and measured by using a hand tally counter. This was repeated for all embryos and all NEO concentrations expect 0.1 mg/L (Flach et al., 2022). To avoid temperature fluctuations, the embryos were adjusted to the room temperature (20 ± 1 °C) for two hours before starting heartbeat measurement.

Analyses of embryo body length, eye area, and heart edema

The embryos were fixed with MEMFAT [0.1 M MOPS (pH 7.4), 2 mM EGTA, 1 mM MgSO4, 4 % formaldehyde, 0.1 % Tween20] at stage 44/45 (Fig. 1A). If more than 20 % of the control embryos died, the entire embryo batch (control and IMD/TMX/CLO-treated embryos) was excluded from the statistical analysis due to likely poor quality of eggs or embryos (Flach et al., 2023b; Seigfried et al., 2017). Four to eight embryo batches were examined under a light microscope (Olympus SZH10 and SZX12, Olympus, Germany) at stage 44/45 for the morphological analyses of the outward appearance (body length, eye area, heart edema). All control embryos within each embryo batch were examined and one representative control embryo was selected for comparison to the other controls and to NEO-exposed embryos (Suppl. Fig. 1A). This was done for each embryo batch. By the respective comparison of the representative control embryo with all embryos of the same embryo batch, the variability that normally exists even in between the control embryos of one embryo batch was included in the evaluation. To perform detailed analyses, two of the most representative morphological analysis experiments that were performed on the respective independent embryo batches were used to measure the body length and eye area (Suppl. Fig. 1B). Each embryo used for the respective experiments was photographed and measured using the Fiji software (Schindelin et al., 2012).

Whole mount in situ hybridization

The embryos were incubated in control and 100 mg/L pesticide solution with each of the NEOs and fixed using MEMFAT at the referring

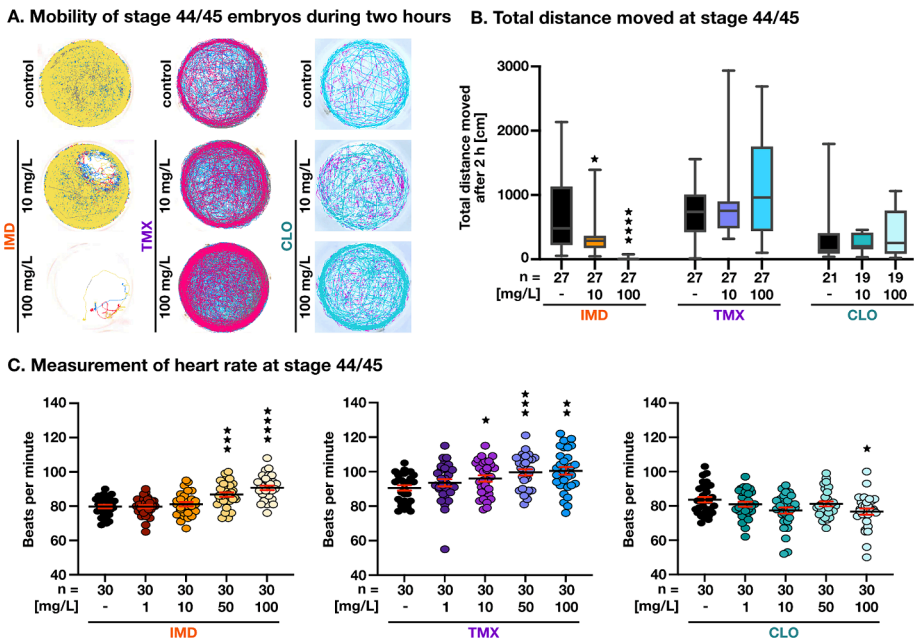

Fig. 2. Influence of IMD, TMX and CLO on the Mobility and Heart Rate of *X. laevis*. A. Mobility of stage 44/45 embryos during two hours. Effect of IMD (left column), TMX (middle column) or CLO (right column) on the embryo's mobility. B. Total distance moved at stage 44/45. The total distance moved by stage 44/45 embryos from two to three embryo batches during two hours was studied. C. Measurement of the heart rate at stage 44/45. The heartbeats of stage 44/45 embryos after exposure to IMD (left panel), TMX (middle panel) or CLO (right panel) were counted for one minute. Abbreviations: IMD, imidacloprid; TMX, thiamethoxam, CLO, clothianidin; mg/L, milligram per liter; cm, centimeter; n, number of embryos analyzed. Statistics: The statistical evaluation always refers to the comparison of the respective exposure group (IMD, TMX, CLO) with the control group (without NEO).

stage as described in section "Exposure of *X. laevis* embryos to IMD, TMX and CLO" (Fig. 1A). Stage 23 was used to study the NCC differentiation and migration as well as the eye-cell differentiation. The cardiomyocyte differentiation was studied at stage 28 and further separation and definition of the cranial placode development (Schlosser, 2006) at stage 32. Cell differentiation and migration were investigated by analyzing the expression of factors required for these developmental processes (Table 1). The gene expression was detected by WMISH approaches according to a standard protocol (Hemmati-Brivanlou et al., 1990). As part of the WMISH, antisense RNA probes were used to detect mRNA activity. For generating the antisense RNA probes, the following plasmids were used: *pax6* (Hollemann et al., 1998) and *rax* (Furukawa et al., 1997) for the eye-cell differentiation, *twist1* (Hopwood et al., 1989) and *egr2* for the NCC migration, *alcam* (Gessert et al., 2008) and *sox3* (Schlosser and Ahrens, 2004) for the cranial placode development, and *actc1* (Gerber et al., 2002) and *mhcα* (Gessert et al., 2008) for the myocardial differentiation. Staining was done using a BM Purple (Roche Diagnostics GmbH, Germany) solution.

The evaluation was performed under a light microscope (Olympus SZH10 and SZX12, Olympus, Germany) by selecting a representative control embryo of each of the four independent embryo batches and comparing it to each embryo in the embryo batch (control and NEO treatment) for gene expression intensity and area (Suppl. Fig. 1A). In addition, the expression intensity and area of *rax* and *mhcα* as well as the length of the *sox3*-expressing cranial placodes were measured for one embryo batch per NEO exposure (Suppl. Fig. 1B) using Fiji software (Schindelin et al., 2012) after each embryo of the respective experiments were photographed. The determined mean expression intensities of the control embryos of one embryo batch were averaged and this mean value was used to normalize all mean expression intensities of the control and treatment groups of the same embryo batch.

Cranial cartilage isolation and measurement

Embryos of *X. laevis* were incubated in the control solution and in 100 mg/L of each NEO solution until they reached stage 45 (see Sections "Exposure of *X. laevis* embryos to IMD, TMX and CLO" and "Analyses of embryo body length, eye area, and heart edema"; Fig. 1A). We performed an Alcian blue staining following an established protocol (Gessert et al., 2007). After the staining, the cartilage (from one embryo batch for each NEO) was manually isolated with two tweezers and analyzed in terms of quantity. To this purpose, the area of the branchial arches was measured bilaterally and averaged and the angle of the Meckel cartilage in the front was detected. Both measurements were carried out using Fiji software (Schindelin et al., 2012) after each isolated cranial cartilage was photographed.

Immunostaining and documentation using confocal microscopy

The cranial nerve (one to three independent embryo batches) and the cardiac structure (two independent embryo batches) of 44/45-stage embryos after the control and pesticide incubations were subjected to immunohistochemical staining with the neuron-specific monoclonal 3A10 antibody (DSHB, USA) and the cardiac troponin T (Tnnt2) antibody (DSHB, USA). Fixation and staining were performed as described before (Schuff et al., 2007).

After each stained embryo was photographed, the optic, trigeminal and mandibular nerves were measured in the 2D images and averaged bilaterally using Fiji software (Schindelin et al., 2012). To examine whether a possible effect of a NEO exposure was nerve-specific, the averaged nerve length data was compared to the root of the embryo head area.

The stained hearts were analyzed and imaged using fluorescence under a stereomicroscope (Olympus MVX10/U-RFL_T with camera UC50, Olympus, Germany) to detect anomalies in the heart structure.

To obtain even more information about the structure of the stained tissue samples, exemplary embryos were imaged as 3D models using a Zeiss LSM710 confocal microscope (Zeiss, Germany) after a 3A10 or Tnnt2 staining process (Flach et al., 2022). Accordingly, the stained embryos were dehydrated with a methanol series trough 100 %

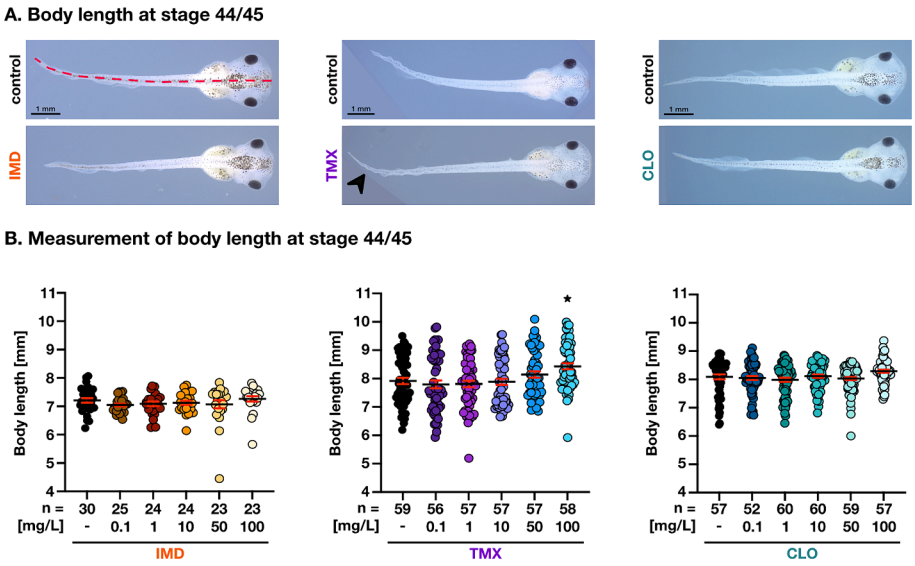

Fig. 3. Effect of IMD, TMX and CLO on the Embryonic Body Length of *X. laevis*. A. Body length at stage 44/45. Dorsal views of embryos at stage 44/45 showed the development of control and NEO-exposed embryos. B. Measurement of body length at stage 44/45. Head-tail length measurements (red dotted line in A) of embryos of one to two representative embryo batches after exposure to IMD (left panel), TMX (middle panel) or CLO (right panel) were compared to control embryos. Abbreviations: IMD, imidacloprid; TMX, thiamethoxam, CLO, clothianidin; mg/L, milligram per liter; mm, millimeter; n, number of embryos analyzed. Statistics: The statistical evaluation always refers to the comparison of the respective exposure group (IMD, TMX, CLO) with the control group (without NEO).

methanol and then placed in MURRAÝs Clear containing 33 % benzyl alcohol (Merk, Germany) and 67 % benzyl benzoate (Merk, Germany) to take images.

Heart isolation and measurements

In order to isolate the heart, 44/45-stage embryos were fixed after incubation (see Sections "Exposure of *X. laevis* embryos to IMD, TMX and CLO" and "Analyses of embryo body length, eye area, and heart edema"; Fig. 1A) and embryos from two to three independent embryo batches from the control and NEO solutions (1, 50, 100 mg/L) were selected. The embryonic hearts were isolated with two tweezers under a light microscope (Olympus SZH10 and SZX12, Olympus, Germany). The photographs were used to measure the width of the atrium and ventricle using Fiji software (Schindelin et al., 2012).

Statistics

The P-values were calculated with a non-parametric, two-tailed Mann-Whitney rank sum test using GraphPad Prism 9 software (San Diego, CA, USA). The error bars represent the standard error of the means (SEM). The statistical significance is indicated as follows: $p > 0.05$, * $p \leq 0.05$, ** $p \leq 0.01$, *** $p \leq 0.001$, **** $p \leq 0.0001$.

Results

IMD, TMX and CLO stability during the experimental exposure time of 14 days

We studied the IMD, TMX and CLO stability during the maximum exposure time of 14 days at 14 °C. No relevant change in the IMD, TMX or CLO concentrations were observed (Fig. 1C). This confirms that the NEOs did not degrade during the specified incubation period and method.

Effect of the NEOs IMD, TMX and CLO on embryonic mobility and heart rate of X. laevis

Exposure to NEOs had a significant effect on the embryonic mobility and heart rate. Incubation in 10 and 100 mg/L IMD resulted in significant decreases in the total distance moved by the embryos (Fig. 2A and B). However, TMX and CLO had no significant effect on the distance moved in the two hours (Fig. 2A and B).

Additionally, all three NEOs altered the heart rate. Imidacloprid (as

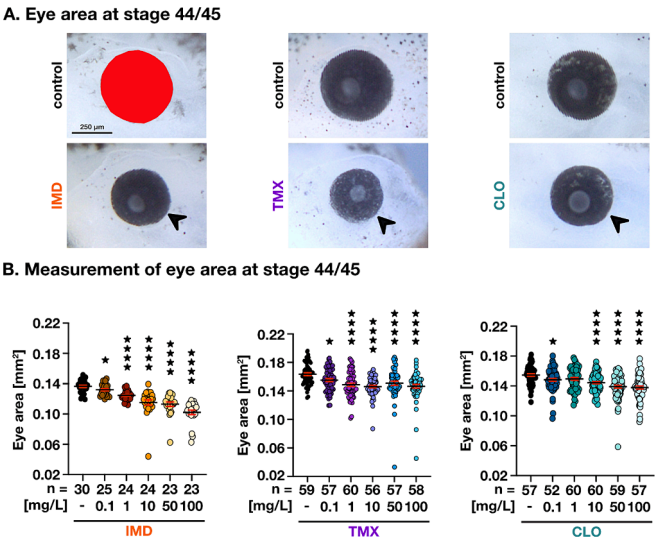

Fig. 4. Effect of IMD, TMX and CLO on the Embryonic Eye Area of *X. laevis*. A. Eye area at stage 44/45. Lateral views of the eyes (black arrowheads show smaller eyes) of control embryos and stage 44/45 embryos after exposure to IMD (left column), TMX (middle column) or CLO (right column). B. Measurement of eye area at stage 44/45. Eye area measurement of one to two representative embryo batches (the area measured is highlighted in red in the control embryo shown in the left corner in A). Comparison of eyes from the control group to eyes after exposure to IMD (left panel), TMX (middle panel) or CLO (right panel). Abbreviations: IMD, imidacloprid; TMX, thiamethoxam, CLO, clothianidin; mg/L, milligram per liter; mm^2, square millimeter; n, number of embryos analyzed. Statistics: The statistical evaluation always refers to the comparison of the respective exposure group (IMD, TMX, CLO) with the control group (without NEO).

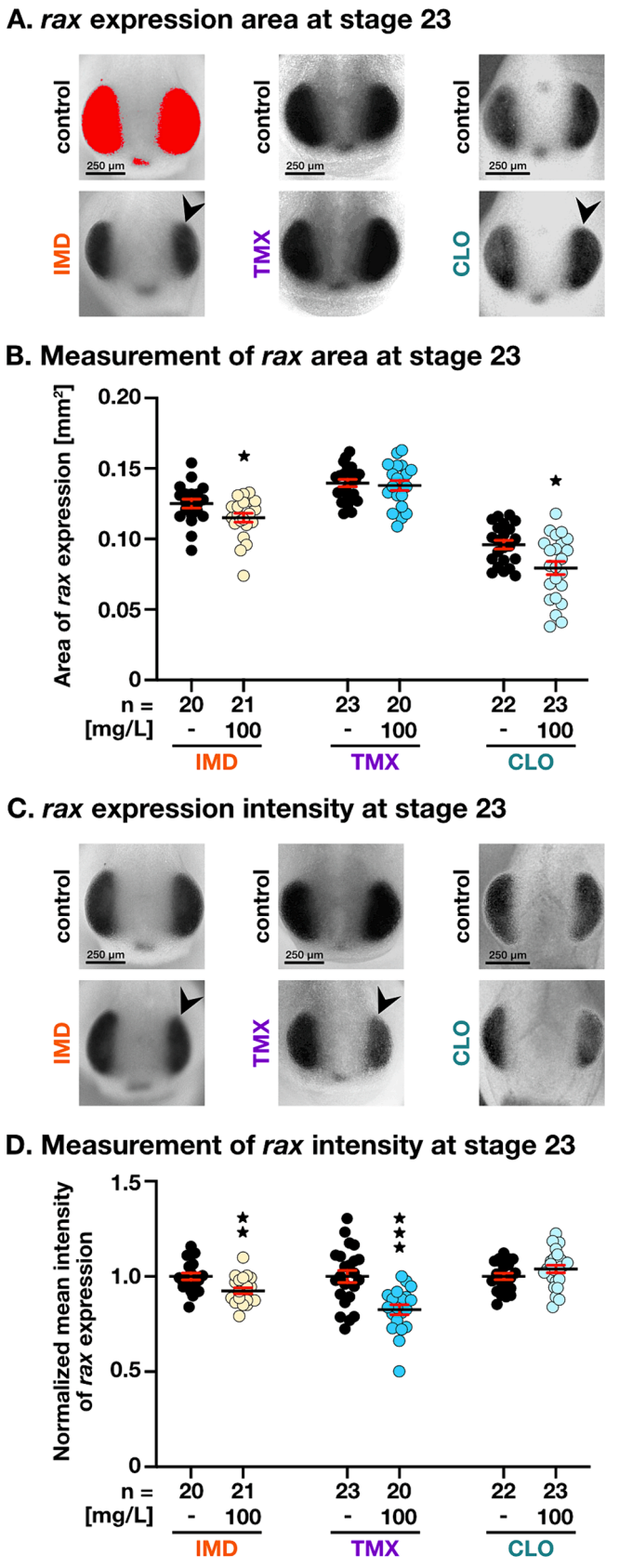

(caption on next column)

Fig. 5. Influence of IMD, TMX and CLO on the Molecular Basis of *X. laevis* Eye Development. A. *rax* expression area at stage 23. Anterior views of the eye-specific gene *rax* at stage 23. Representative images of the expression area (highlighted in red) after exposure to IMD (left column), TMX (middle column) or CLO (right column) compared to control embryos. The area of IMD- and CLO-treated embryos is reduced (black arrowheads). B. Measurement of *rax* area at stage 23. Quantification of the total expression area of the eye-specific gene *rax* of one embryo batch. C. *rax* expression intensity at stage 23. Anterior views of the eye-specific gene *rax* at stage 23. Representative images showing the intensity of the *rax* expression. Less intense expression is measured after an exposure to IMD and TMX (black arrowheads). D. Measurement of *rax* intensity at stage 23. Statistical evaluation of the normalized mean intensity of *rax* expression of one embryo batch. Abbreviations: IMD, imidacloprid; TMX, thiamethoxam, CLO, clothianidin; mg/L, milligram per liter; mm^2, square millimeter; n, number of embryos analyzed. Statistics: The statistical evaluation always refers to the comparison of the respective exposure group (IMD, TMX, CLO) with the control group (without NEO).

of 50 mg/L) and TMX (as of 10 mg/L) significantly increased the heart rate (Fig. 2C, left and middle panel), while CLO (100 mg/L) reduced the heart rate (Fig. 2C, right panel).

Effect of the NEOs IMD, TMX and CLO on mortality and body length of X. laevis

Based on four to eight independent embryo batches per NEO concentration through 100 mg/L, none of the three NEOs (IMD, TMX, CLO) affected the mortality rate of *X. laevis* embryos (Suppl. Fig. 2).

A significant increase in body length was observed in embryos (n = 23–69) incubated in 100 mg/L TMX (Fig. 3A and B, middle panel). Neither of the lower TMX concentrations nor an incubation in the other two NEOs (IMD and CLO) resulted in a significant change in body length (Fig. 3A and B, left and right panel).

Incubation in IMD, TMX and CLO impairs eye development

A significant reduction of the eye area of stage 44/45 embryos was found for each NEO studied and at each concentration (Fig. 4A and B).

To analyze a possible molecular basis for the eye phenotype, four embryo batches (n = 81–96) at stage 23, when eye cells differentiate, were used for an WMISH of the eye-cell specific genes *pax6* and *rax*, but no significant change was observed (data not shown). To perform a more detailed analysis, the area and intensity of the *rax* expression of all embryos (n = 20–23) from one representative embryo batch at each concentration were measured. No changes in the *rax* expression area were observed after an exposure to TMX, whereas the area was reduced after an exposure to IMD and CLO (Fig. 5A and B). In contrast, IMD and TMX resulted in a reduced intensity of the *rax* expression, whereas CLO had no effect on the *rax* intensity (Fig. 5C and D).

All three NEOs cause structural changes to the cranial cartilage

The overall appearance of the cranial cartilage changed after an incubation in all three NEOs (Fig. 6A). The cartilage showed visible deformations starting at 1 mg/L (IMD and CLO) or 50 mg/L (TMX) (Fig. 6A). The branchial arch areas decreased (Fig. 6B), and the angle of the Meckel cartilage became more acute (n = 19–28). (Fig. 6C).

All three NEOs impact cranial nerve and placode development

The cranial nerves of stage 45 embryos were examined in 2D after their incubation in 100 mg/L of a NEO solution (n = 20–74) (Fig. 7A and B). To check the specificity of the nerve length, it was compared to the root of the head area, which made it possible to determine whether the nerves are shorter simply due to the smaller head or whether the nerves are shorter regardless of the size of the head. The measurements showed

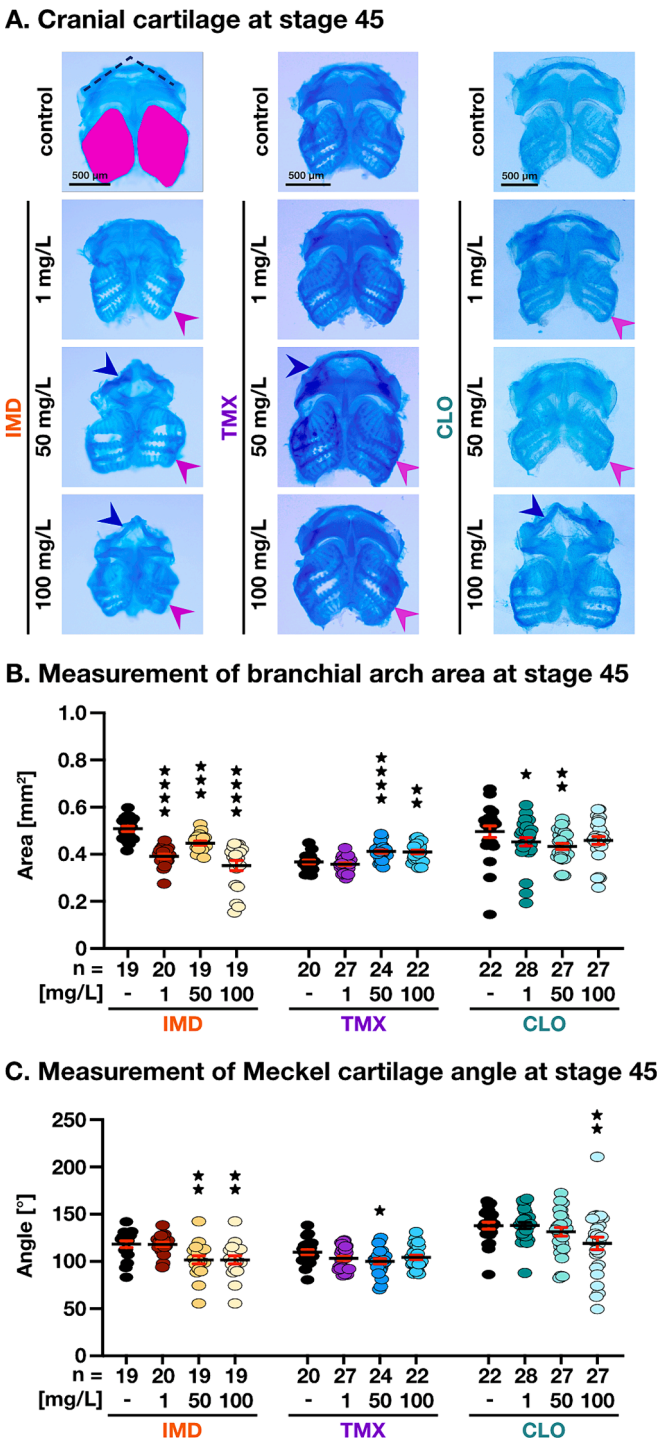

Fig. 6. Cranial Cartilage Development of *X. laevis* after Exposure to IMD, TMX or CLO. A. Cranial cartilage at stage 45. Exposure to IMD (left column), TMX (middle column) and CLO (right column) resulted in changes in branchial arch area (pink arrowheads) and to a deformation and tightening of the Meckel cartilage angles (blue arrowheads) at stage 45. B. Measurement of the branchial arch area at stage 45. Branchial arch area measurement (measurement as by pink area in the left control in A). Both sides of one embryo batch were measured and the average value was determined. C. Measurement of Meckel cartilage angle at stage 45. The angle (blue dotted line in A) of the Meckel cartilage of one embryo batch was measured. Abbreviations: IMD, imidacloprid; TMX, thiamethoxam, CLO, clothianidin; mg/L, milligram per liter; mm^2, square millimeter; °, degrees; n, number of embryos analyzed. Statistics: The statistical evaluation always refers to the comparison of the respective exposure group (IMD, TMX, CLO) with the control group (without NEO).

that IMD and CLO had caused a highly significant shortening of the *Nervus opticus* (pink), the *Nervus trigeminus* (blue) and the *Nervus mandibularis* (turquoise) (Fig. 7A and B). An exposure to TMX did not significantly change the length of any of the nerves (Fig. 7B).

A more detailed inspection with a confocal microscope revealed structural differences in the appearance of the optic nerve with regard to all three NEOs (Fig. 7C). In addition, the entire structure of the nerves seemed to be fibrous and impaired, especially after an exposure to CLO (Fig. 7C).

Both the cranial cartilage and the cranial nerves are derivatives of NCCs. To study earlier developmental stages in more detail, we used NCC-specific genes and performed WMISH experiments at stage 23 (NCC differentiation and migration). The microscopic examination showed that the NCC-specific genes *twist1* and *egr2* were not significantly altered in the expression patterns in stage 23 embryos after their exposure to any of the NEOs (n = 81–102) (data not shown).

Cranial nerves also partially develop from the cranial placodes, which is why the cranial placode development was analyzed through WMISH experiments using the tissue-specific genes *alcam* and *sox3*. It was found that IMD, TMX and CLO have an effect on the development of cranial placodes. While the analysis of the specific gene *alcam* (n = 86–110) showed a significant change in expression after an exposure to TMX or IMD, an exposure to CLO only resulted in statistically insignificant changes (Suppl. Fig. 3A and B). The opposite is true for the second gene studied, *sox3* (n = 85–105). The NEOs IMD and CLO significantly altered the expression pattern, whereas TMX only resulted in statistically insignificant changes (Suppl. Fig. 3C and D). Length measurements of the epibranchial placodes from one embryo batch (n = 22–29) confirmed the changes in the *sox3* expression caused by the NEOs (Fig. 8A and B). The TMX exposure led to a shorter epibranchial placode IX (Fig. 8B, middle panel), and IMD and CLO resulted in a shortening of the epibranchial placode X (Fig. 8B, lower panel). None of the three NEOs altered the *sox3* expression in the epibranchial placode VII (Fig. 8B, upper panel).

All three NEOs impacted cardiac parameters

Since it had already been determined that all three NEOs have an effect on the heart rate (Fig. 2C), we examined the cardiac region and the heart in detail. During this microscopic examination, we were able to detect heart edema in four to eight embryo batches at higher (10–50 mg/L) NEO concentrations following an incubation in all three NEOs (n = 110–231) (Fig. 9A and B).

Likewise, contact with the NEOs affected the structure of the heart. Some isolated hearts had wider atria and ventricles (Fig. 10A). Exposure to IMD (at 50 mg/L) and TMX (at 1 and 50 mg/L) resulted in larger atria, while the size of the atria normalized at 100 mg/L. An exposure to CLO had no significant effect on the width of the atria (Fig. 10B). The ventricle became enlarged after incubation in all three NEOs (IMD and CLO from 50 mg/L, TMX at 50 mg/L) (Fig. 10C).

The structural difference is also evident in immunostaining using the Tnnt2 antibody in whole embryos (Fig. 11A). An exposure to IMD resulted in abnormal hearts in 78.00 % (50 mg/L) and 86.36 % (100 mg/L) of the embryos examined (n = 44–52) (Fig. 11A, left column). In contrast, the other two NEOs had a less significant effect on the heart structure (TMX, Fig. 11A, middle column: 24.07 % (50 mg/L), 21.67 % (100 mg/L), (n = 108–120); CLO, Fig. 11A, right column: 26.92 % (50 mg/L), 54.35 % (100 mg/L), (n = 46–53)).

In addition, we observed structural changes using 3D models and their virtual cross sections (Fig. 11B). Randomly selected embryos were found to have less structured ventricle (v), atria (a) and outflow tract (oft) walls after having been exposed to IMD, TMX or CLO.

At the molecular level, we analyzed the expression pattern of the cardiac-specific genes *actc1* and *mhcα* at stage 28. The analyses that were performed with a light microscope revealed no abnormal expression patterns of both genes for all three NEOs (n = 82–100) (data not shown).

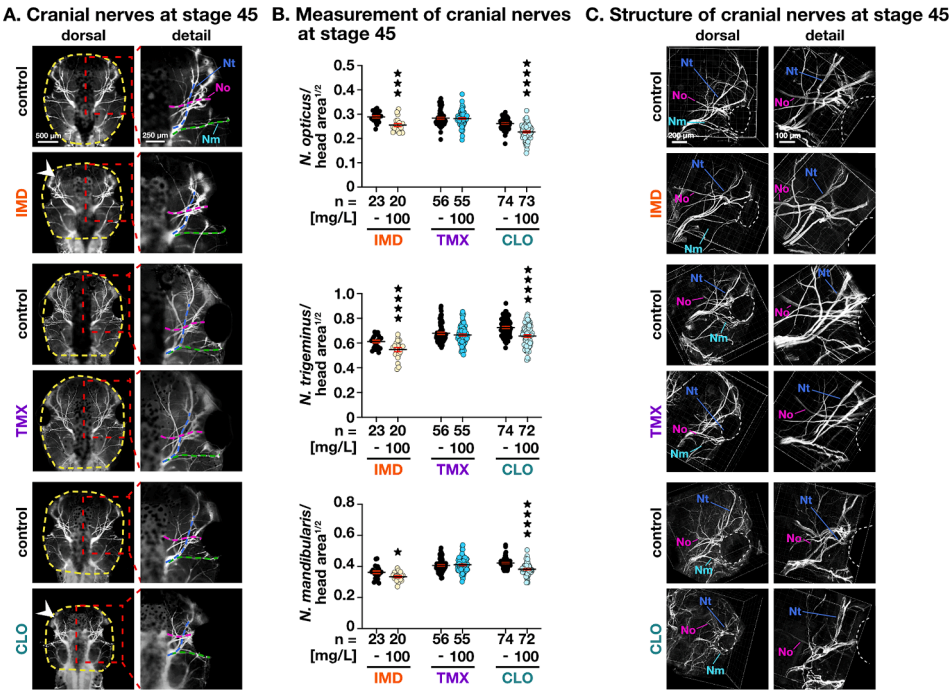

Fig. 7. Effect of IMD, TMX and CLO on the Cranial Nerve Development. A. Cranial nerves at stage 45. Dorsal views of IMD, TMX or CLO-treated embryos compared to control embryos at stage 45 made visible through 3A10 antibody staining. B. Measurement of cranial nerves at stage 45. Quantification of the ratios between the cranial nerve length to the root of the head area (yellow dotted circle in A) at stage 45 after an exposure of one to three embryo batches to IMD, TMX or CLO. Statistical evaluations of the lengths of *N. opticus* (pink dotted lines in A), *N. trigeminus* (blue dotted lines in A) and *N. mandibularis* (green dotted lines in A) are performed. C. Detailed structure of cranial nerves at stage 45. Dorsal overview and detailed imaging of 3D models of the stained cranial nerves are shown. Cranial nerves appear thinner and less structured after exposure to IMD, CLO and TMX. Abbreviations: IMD, imidacloprid; TMX, thiamethoxam, CLO, clothianidin; No, *Nervus opticus*; Nt, *Nervus trigeminus*; Nm, *Nervus mandibularis*; mg/L, milligram per liter; mm, millimeter; n, number of embryos analyzed. Statistics: The statistical evaluation always refers to the comparison of the respective exposure group (IMD, TMX, CLO) with the control group (without NEO).

We also quantified the *mhcα* expression area and intensity using one representative embryo batch per NEO (n = 17–29). The expression area showed no change for any pesticide (Fig. 12A and B), whereas the *mhcα* expression intensity decreased significantly after an exposure to TMX and CLO (Fig. 12C and D).

Discussion

Relevance of our study

Pesticides including the insecticides of the NEO group are used worldwide and in large quantities (Environmental Fate and Effects Division Office of Pesticide Programs, 2023; Miles et al., 2017; YongFan, 2015). Yet, their effects on non-target organisms have not been widely studied. The South African clawed frog *X. laevis* was used in this study to examine the possible effects of different NEOs (IMD, TMX, CLO) on the early embryogenesis of an aquatic organism. We observed several negative effects (external appearance, swimming mobility, neural and cardiac embryonic development). Some parameters were significantly altered upon exposure to as little as 0.1 mg/L of all three NEOs (IMD, TMX, CLO).

The concentrations we used reflect NEO concentrations that already have been measured in nature (Chrétien et al., 2017; Miles et al., 2017; Van Dijk et al., 2013), as well as "worst-case" scenarios that are intended to provide detailed information about the effects of an incorrect use or disposal of NEOs on aquatic organisms. Even the liquid droplets (guttation droplets) secreted by seed-treated plants have very high concentrations of NEO residue (up to 100 mg/L TMX and CLO and even 200 mg/L IMD), which means that the possibility that non-target organisms will come in contact with such high NEO concentrations in nature cannot be ruled out (Girolami et al., 2009).

Furthermore, the tests relating to this study were conducted under laboratory conditions that were free of external threats such as temperature fluctuations, the presence of multiple pesticides, other contaminants, or predators. Such combinations may amplify the effects of individual NEOs that were observed. In addition, even small developmental defects or delays could have serious consequences for the survival of animals in nature. To test this hypothesis, field studies should be carried out to include natural conditions.

Stability of IMD, TMX and CLO in solutions

The NEOs used here were stable in the solutions under our laboratory conditions during the 14 days of incubation and light conditions corresponding to a natural day/night cycle. Lu et al. (2015) investigated the half-lives of these NEOs in surface waters at 50°N latitude for spring, summer, autumn, and winter by sunlight on clear days. Depending on the season, the values varied from 0.36 to 2.22 days for IMD, from 0.20 to 1.49 days for TMX and from 0.35 to 3.31 days for CLO (Lu et al., 2015). The results of other studies indicate longer half-lives of NEOs (IMD: up to 20 days (Zheng and Liu, 1999); TMX: up to 29.2 days (Karmakar et al., 2009)) in aqueous solutions. This difference shows the dependency of the half-lives are on various factors such as solar radiation, water temperature and pH value (Karmakar et al., 2009; Todey et al., 2018; Zheng and Liu, 1999).

Different effects of IMD, TMX and CLO on embryo mobility and heart rate

The fact that IMD leads to a reduction in mobility has already been substantiated in studies on other organisms across the phylogenetic tree, such as white-tailed deer (*Odocoileus virginianus*), freshwater shrimp (*Neocaridina denticulata)* or mayfly nymphs *(Gammarus pulex*) (Berheim et al., 2019; Roessink et al., 2013; Siregar et al., 2021). In our earlier studies, we demonstrated a reduction in the mobility of *X. laevis* embryos

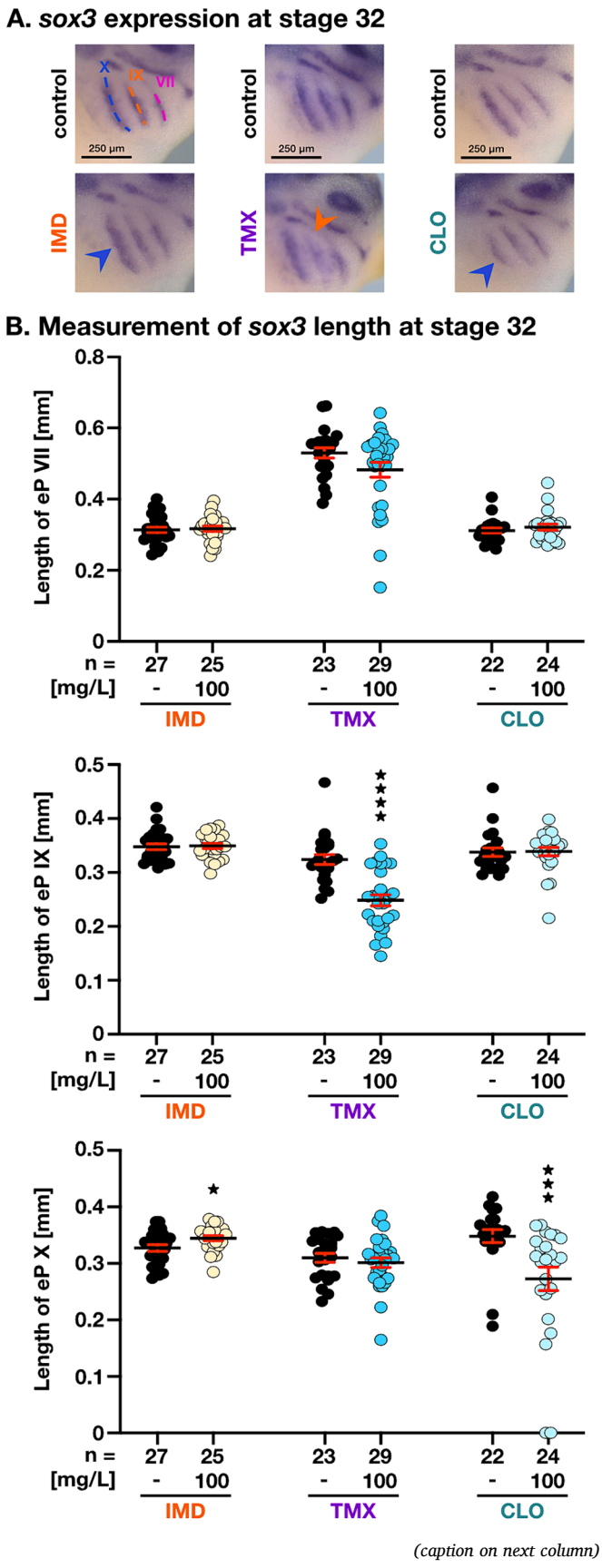

(caption on next column)

Fig. 8. Effect of IMD, TMX and CLO on the Expression of the Cranial Placode-Specific Gene *sox3*. A. *sox3* expression at stage 32. Lateral view of embryos after WMISH staining with the cranial placode-specific gene *sox3* showing the epibranchial placodes VII (pink dotted line), IX (orange dotted line) and X (blue dotted line). B. Measurement of *sox3* expression lengths at stage 32. Length measurement of the different epibranchial placodes of one embryo batch. IMD and CLO lead to changes in the length of eP X (blue arrowhead in A), and TMX to a shortening of eP IX (orange arrowhead in A). Abbreviations: IMD, imidacloprid; TMX, thiamethoxam, CLO, clothianidin; eP, epibranchial placode; mg/L, milligram per liter; mm, millimeter; n, number of embryos analyzed. Statistics: The statistical evaluation always refers to the comparison of the respective exposure group (IMD, TMX, CLO) with the control group (without NEO).

after exposure to the NEOs thiacloprid (Flach et al., 2023b) and acetamiprid (Kerner et al., 2023) similar to IMD shown in our study here. In contrast to our results here, individual studies have shown that TMX and CLO effect mobility of rainbow trout embryos (Finnegan et al., 2017; Hayasaka et al., 2012). One possible explanation for the mobility effect of NEOs could be a neuronal transmitter imbalance caused by NEOs since an administration of CLO to the striatal regions of rats resulted in a release of dopamine (Faro et al., 2019). Various studies have furthermore shown that NEOs can lead to decreased acetylcholinesterase (AChE) activity, which results in a relative acetylcholine overdose (Jenkins et al., 2021). This condition could be associated with lower agility levels, which, as has been documented, is an aspect of the pathogenesis of akinetic Parkinsońs disease in humans (Győri et al., 2017; Jemec et al., 2007; Radwan and Mohamed, 2013). In addition, NEOs seem to have different effects on the neuronal transmitter release and enzyme activity depending on the dose. For example, lower doses of CLO (0.2 mg/L) increased the AChE levels in the liver of juvenile *X. laevis*. In contrast, 1 mg/L CLO decreased the AChE levels (Jenkins et al., 2021).

The increased heart rate after an exposure to IMD and TMX is consistent with the results of previous studies analyzing the NEO thiacloprid in *X. laevis* (from 50 mg/L) (Flach et al., 2023b) or zebrafish embryos (1 mg/L) (Osterauer and Köhler, 2008). The change in the heart rate could be due to the fact that the metabolism is trying to eliminate the toxic substance (Osterauer and Köhler, 2008). The chemical relationship between IMD, TMX, and nicotine could be another reason for the increased heart rate since nicotine leads to the release of catecholamines. This, in turn, leads to vasoconstriction and an increased heart rate (Benowitz, 2009). In contrast, an exposure to CLO resulted in a decrease heart rate that was similar to the decrease previously shown in zebrafish in connection with an exposure to acetamiprid, which is a NEO as well (Ma et al., 2019).

Effect of TMX on the body length of X. laevis

The unchanged body length of *X. laevis* following exposure to IMD and CLO is consistent with studies on embryos of other frog species (*Lithobates sylvaticus; Lithobates pipiens*), sockeye salmon (*Oncorhynchus nerka*), and the larvae of northwestern salamanders (*Ambystoma gracile*) (Danis and Marlatt, 2021; Marlatt et al., 2019; Robinson et al., 2019). In contrast to the increased body length observed following exposure to 100 mg/L TMX in our study, a previous study using TMX (0.01 to 100 mg/L) on zebrafish showed no effects (Liu et al., 2018). A study on *X. laevis* at the pre-metamorphic stage described smaller embryos following an exposure to 20 mg/L CLO (Jenkins et al., 2021), which also differs from the results of this study. This suggests the importance of the timing and developmental stage at which NEO exposure occurs and offers a possible explanation for the difference between our findings and previous results.

IMD, TMX and CLO effect eye development of X. laevis

The compounds studied resulted in significantly smaller eyes. It has

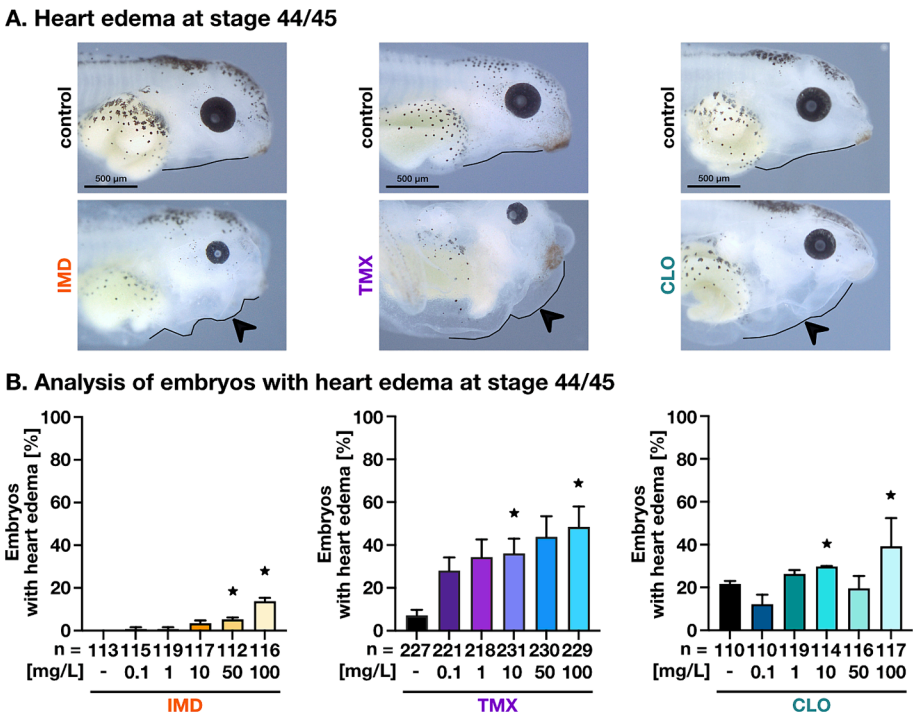

Fig. 9. Effect of an Exposure to IMD, TMX and CLO on the Development of Heart Edema in *X. laevis*. A. Heart edema at stage 44/45. Exposure to IMD (left column), TMX (middle column) and CLO (right column) led to the formation of heart edema (black arrowheads) at stage 44/45. B. Analysis of embryos with heart edema at stage 44/45. Statistical evaluation of embryos with heart edema from four independent embryo batches. Abbreviations: IMD, imidacloprid; TMX, thiamethoxam, CLO, clothianidin; mg/L, milligram per liter; n, number of embryos analyzed. Statistics: The statistical evaluation always refers to the comparison of the respective exposure group (IMD, TMX, CLO) with the control group (without NEO).

previously been found that IMD has a negative effect on the eye development of zebrafish embryos (Tišler et al., 2009) and that the NEOs thiacloprid and acetamiprid lead to smaller eyes in *X. laevis* embryos (Flach et al., 2023b; Kerner et al., 2023). At the molecular level, a reduced expression of *pax6* due to IMD was found in chick embryos (Liu et al., 2016) and a reduced expression of *rax* due to the NEO thiacloprid in *X. laevis* embryos (Flach et al., 2023b). In this study, we did not detect any changes in the *pax6* expression, but in the *rax* expression for all three NEOs. The reduced *rax* expression might correlate with the reduced area of the fully developed eyes at later stages. It is already known that the gene *rax* serves as an important transcription factor for the retinal and optic nerve development (Muranishi et al., 2012) and that a homozygous mutation of *rax* results in anophthalmia in humans (Abouzeid et al., 2012).

IMD, TMX and CLO lead to changes in neural tissue development

Analyses performed on the brains of mice in previous studies have made it clear that orally administered TMX and CLO can reach the central nervous system (CNS) (Ford and Casida, 2006). Therefore, it is conceivable that these NEOs can damage brain functions and the development of the brain. Metabolic enzymes in the brain tissue of premetamorphotic *X. laevis* frog showed changes in activity after contact with CLO (Jenkins et al., 2021). The CNS tissues examined in this study were the cranial cartilage and cranial nerves, which showed severe abnormalities and structural changes after contact with each of the three NEOs. Both tissues develop from NCCs (Crane and Trainor, 2006). The NEO IMD (500 µM = approximately 0.0023 mg) affects the NCC development in chick embryos, a fact that aligns well with our findings. Exposure to IMD also resulted in craniofacial deformations of chick embryos (Wang et al., 2016), which is consistent with the deformation of the cranial cartilage of *X. laevis* in our study. Although WMISH did not reveal any relevant changes in the expression of the NCC-specific genes *twist1* and *egr2* in stage 23 embryos in our study, developmental abnormalities in the NCC formation may still be possible.

Cranial nerves develop partly from NCCs and partly from cranial placodes (Schlosser and Northcutt, 2000). Approaches of WMISH performed with the cranial placode-specific genes *alcam* and *sox3* revealed molecular differences in placodes IX (TMX) and X (IMD and CLO). In particular, the two NEOs IMD and CLO caused a shortening of the optic and trigeminal nerves. Despite the effects on the placode development, the nerves that were measured following an exposure to TMX had not become shorter. This could be due to the difference between the placodes that we analyzed molecularly and those from which the measured nerves developed. Another explanation is that the NEOs may not only have caused the shortening but also structural changes, which we cannot detect by measuring the length. The fact that NEOs can cause structural changes in the nervous tissue of marsh frogs (*Rana ridibunda*) has been substantiated (Çamlıca et al., 2019).

Contact with IMD, TMX and CLO results in an abnormal cardiac development

Various studies have shown that NEOs may influence the production of important enzymes necessary for the oxidative stress regulation such as superoxide dismutase, catalase or glutathione-s-transferase (Jemec et al., 2007; Malev et al., 2012; Qi et al., 2018). This can lead to membrane defects, changes in gene expression, and cellular damage and thereby also cause edema, which were observed after an exposure to any of the three NEOs. Moreover, different studies have shown that NEOs can lead to structural changes in the heart in frog, zebrafish and chicken (Flach et al., 2023b; Gao et al., 2016; Kerner et al., 2023; Zhong et al., 2021).

In addition, TMX and CLO lead to significant changes in the *mhcα* expression. This observation suggests that the early negative effect of TMX and CLO on cardiac cell differentiation is one explanation for the altered cardiac development in *X. laevis* embryos. Mutations in *MHCα* have also been found in human patients with hypertrophic and dilated

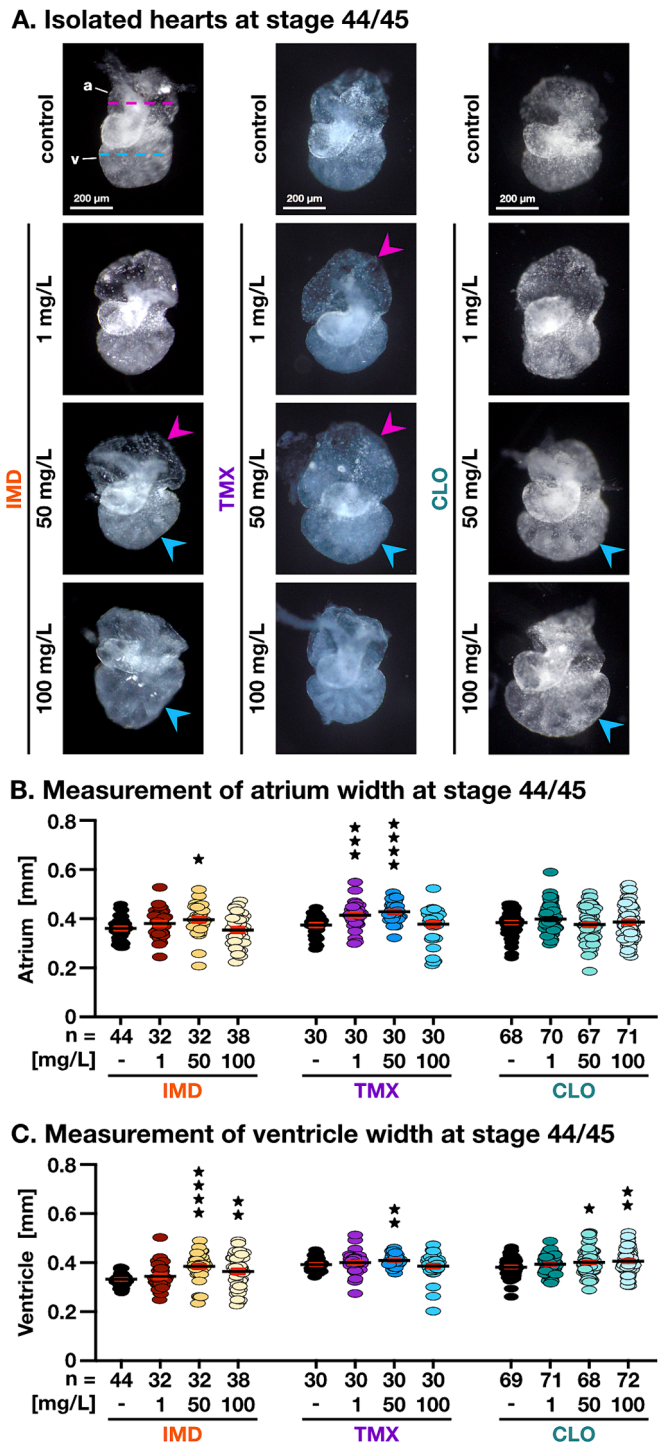

Fig. 10. Effect of IMD, TMX and CLO Exposure on the Heart Size of *X. laevis*. A. Isolated hearts at stage 44/45. Images of isolated hearts after an exposure to IMD (left column), TMX (middle column) and CLO (right column) compared to control hearts. Atria (pink arrowheads) and ventricles (turquoise arrowheads) appear wider. B. Measurement of atrium width at stage 44/45. Measurement of atrial width (pink dotted line in A) after IMD, TMX and CLO incubation. C. Measurement of ventricle width at stage 44/45. Measurement of the ventricle width (turquoise dotted line in A) was also performed. Abbreviations: IMD, imidacloprid; TMX, thiamethoxam, CLO, clothianidin; mg/L, milligram per liter; mm, millimeter; n, number of embryos analyzed. Statistics: The statistical evaluation always refers to the comparison of the respective exposure group (IMD, TMX, CLO) with the control group (without NEO).

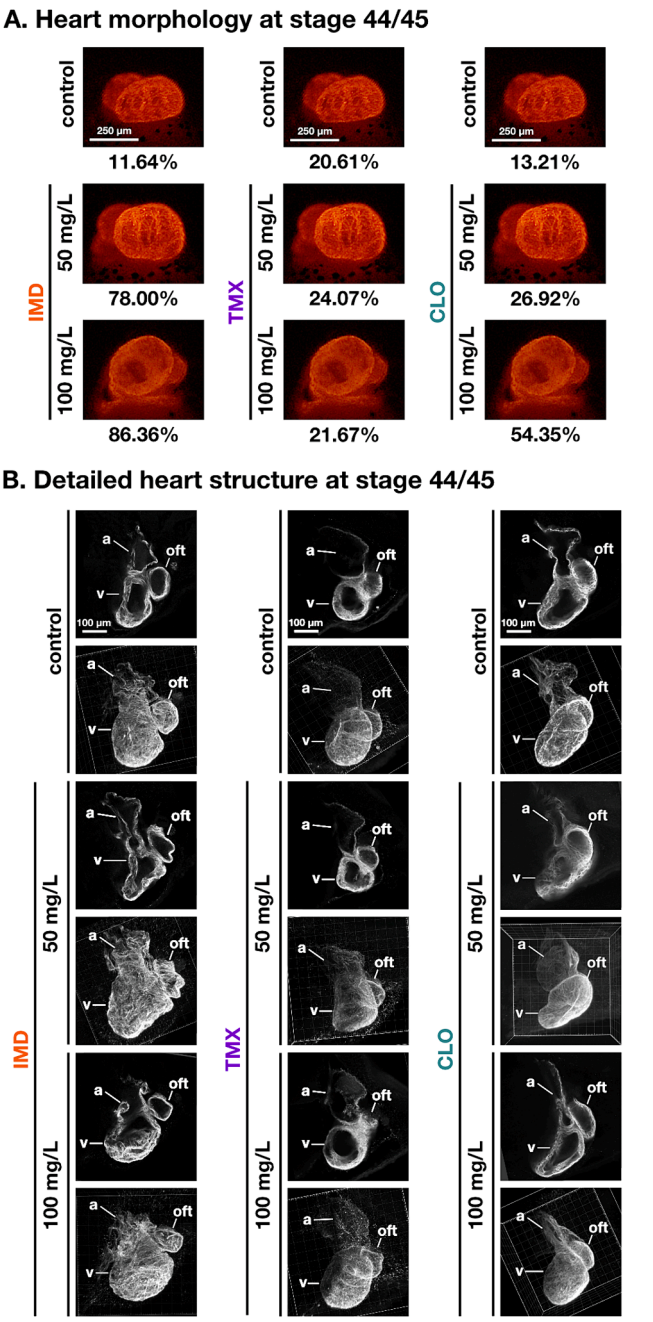

Fig. 11. Structural Analyses of *X. laevis* Cardiac Development after IMD, TMX and CLO Exposure. A. Heart morphology at stage 44/45. Ventral views of the hearts in the embryos from two embryo batches after Tnnt2 antibody staining at stage 44/45. The percentages stated indicate the proportion of embryos with an abnormal heart structure (IMD: control: 11.64 % of 52 embryos, 50 mg/L: 78.00 % of 50 embryos, 100 mg/L: 86.36 % of 44 embryos; TMX: control: 20.61 % of 58 embryos, 50 mg/L: 24.07 % of 54 embryos, 100 mg/L: 21.67 % of 60 embryos; CLO: control: 13.21 % of 53 embryos, 50 mg/L: 26.92 % of 52 embryos, 100 mg/L: 54.35 % of 46 embryos). B. Detailed heart structure at stage 44/45. Detailed analysis of the heart structure of randomly selected embryos using the confocal microscope. The sections and 3D models of the heart are shown for each NEO and each concentration. The heart muscle tissue appears deformed and less organized at higher NEO concentrations. Abbreviations: IMD, imidacloprid; TMX, thiamethoxam, CLO, clothianidin; a, atrium; v, ventricle; oft, outflow-tract; mg/L, milligram per liter; n, number of embryos analyzed. Statistics: The statistical evaluation always refers to the comparison of the respective exposure group (IMD, TMX, CLO) with the control group (without NEO).

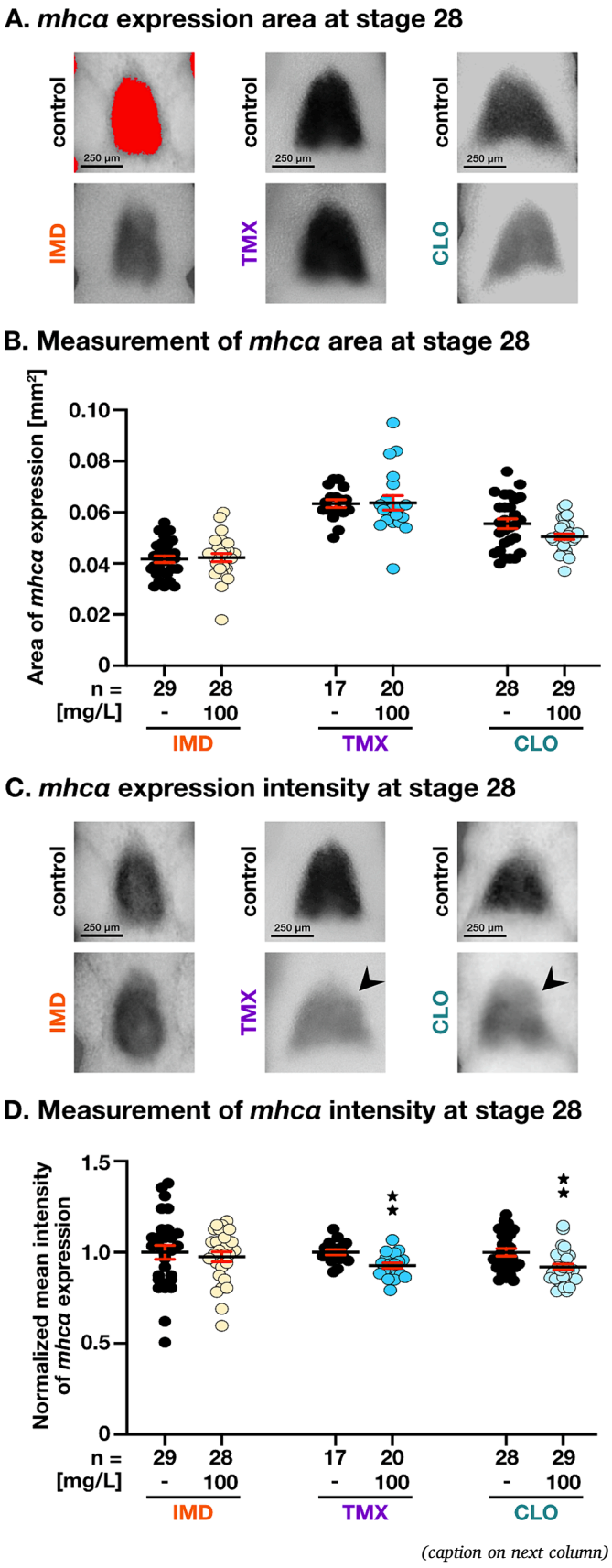

(caption on next column)

Fig. 12. Molecular Basis of *X. laevis* Cardiac Development after Exposure to IMD, TMX and CLO. A. *mhcα* expression area at stage 28. Area of expression of the cardiac-specific gene *mhcα* at stage 28. The area of expression is shown in red. B. Measurement of *mhcα* area at stage 28. Statistical analysis of *mhcα* expression area after exposure to IMD, TMX and CLO. C. *mhcα* expression intensity at stage 28. Ventral views of the intensity of *mhcα* expression at stage 28. The black arrowheads show a reduced intense expression after exposure to TMX and CLO. D. Measurement of *mhcα* intensity at stage 28. Normalized mean intensity of *mhcα* expression. Abbreviations: IMD, imidaclopridi; TMX, thiamethoxam, CLO, clothianidin; mg/L, milligram per liter; mm^2, square millimeter; n, number of embryos analyzed. Statistics: The statistical evaluation always refers to the comparison of the respective exposure group (IMD, TMX, CLO) with the control group (without NEO).

cardiomyopathy, resulting in a decreased systolic pumping force and loss of ejection fraction (Granados-Riveron et al., 2010). This represents a possible explanation for the altered heart rate after an exposure to any of the three NEOs in this study. Further studies are needed to prove this hypothesis. Structural abnormalities in cardiac tissue associated with an altered heart rate could potentially be an indicator of heart failure accompanied by inadequate tissue perfusion and oxygenation.

Possible relationship between the organ and tissue defects caused by an exposure to IMD, TMX and CLO

The question arises as to whether there could be correlations between the different organ and tissue defects caused by an exposure to IMD, TMX or CLO.

It is already known with regard to human diseases with complex symptoms that there can be links between craniofacial malformations and heart defects (e.g., Di George syndrome or CHARGE syndrome), eye development disorders (e.g., Waardenburg syndrome or Axenfeld-Rieger syndrome) or autonomic nervous system disorders (e.g. familial dysautonomia) (Vega-Lopez et al., 2018). All these syndromes belong to the large group of neurocristopathies caused by NCC development defects (Vega-Lopez et al., 2018) including abnormalities of the eye (Williams and Bohnsack, 2015), the cranial cartilage/nerves (Le Douarin et al., 2007; Lee et al., 2003) and the heart (Cavanaugh et al., 2015). Since NEOs are already associated with NCC development defects (Cerrizuela et al., 2020) and we were able to detect defects in the cranial placode-specific gene expression as well, the effect of NEOs on the NCC/cranial placode development may be a cause of the various defects in *X. laevis*.

Another plausible correlation between the various changes would be the influence of oxidative stress, which can affect embryonic development by impacting the gene expression and signaling as well as changes in the cell cycle (Dennery, 2007), as a result of which dysmorphia or edema could develop in various tissues. Several studies have already shown that NEOs influence enzymes that are important for the regulation of oxidative stress (Jemec et al., 2007; Malev et al., 2012; Qi et al., 2018). These results support the assumption that oxidative stress could be a cause for the different effects of NEOs in *X. laevis*.

In addition, studies have already shown that embryos are more susceptible to harmful substances at early development stages (Ortiz-Santaliestra et al., 2006), which would further explain the wide-ranging effects of NEOs at this stage. This study showed that the structure and function of the heart were significantly altered after NEO exposure. These changes and functional limitations could have led to a general deficit of critical nutrients due to a lack of blood circulation in the organism and could thus also be an additional cause of the effects on the various organs and tissues.

Conclusion

A comparison of the three NEOs shows that IMD has the strongest effect on *X. laevis* embryogenesis, because an exposure to IMD leads to

negative effects in all organs and tissues studied (eyes, cranial cartilage, cranial nerves, and heart). Most importantly, IMD leads to a drastic reduction in mobility up to complete immobility, which is a major problem in nature in terms of foraging and escape from predators.

The NEO CLO particularly affects the development of the eyes, cranial cartilage, and cranial nerves. The NEO TMX does not affect the cranial cartilage and nerves as much, but it has a greater effect on the heart development than CLO. Especially interesting is the fact that although CLO is a metabolite of TMX, the two substances are not very similar in their effects. This underscores the fact that metabolites of pesticides pose a risk to the environment in their own right and should therefore also be taken into account in the registration of compounds.

Thus, the effects of TMX and CLO compared to IMD are not only different, but in some respects even opposite to each other, suggesting different modes of action that should be clarified in the future, with considerations in aquatic species of life stage, NEO concentration, and exposure duration.

Since there are strong effects on the development of the *X. laevis*, a strict and frequent monitoring of pesticide levels, and those of their metabolites, in the environment would provide important environmental benchmarks.

Declaration of competing interest

The authors declare that they have no known competing financial interests or personal relationships that could have appeared to influence the work reported in this paper.

Data availability

Data will be made available on request.

Acknowledgements

We would like to thank Ute von Wietersheim (Certified Translator German-English) for her editing assistance with the manuscript.

Appendix A. Supplementary data

Supplementary data to this article can be found online at https://doi.org/10.1016/j.crtox.2024.100169.

References

Abouzeid, H., Youssef, M.A., Bayoumi, N., ElShakankiri, N., Marzouk, I., Hauser, P., Schorderet, D.F., 2012. RAX and anophthalmia in humans: Evidence of brain anomalies. Molecular Vision. 18, 1449-1456. PMID: 22736936; PMCID: PMC3380941.

Andreazzoli, M., Gestri, G., Cremisi, F., Casarosa, S., Dawid, I.B., Barsacchi, G., 2003. Xrx1 controls proliferation and neurogenesis in *Xenopus* anterior neural plate. Development 130, 5143–5154. https://doi.org/10.1242/dev.00665.

Benowitz, N.L., 2009. Pharmacology of nicotine: Addiction, smoking-induced disease, and therapeutics. Annu. Rev. Pharmacol. Toxicol. 49, 57–71. https://doi.org/10.1146/annurev.pharmtox.48.113006.094742.

Berheim, E.H., Jenks, J.A., Lundgren, J.G., Michel, E.S., Grove, D., Jensen, W.F., 2019. Effects of neonicotinoid insecticides on physiology and reproductive characteristics of captive female and fawn white-tailed deer. Sci Rep 9, 4534. https://doi.org/10.1038/s41598-019-40994-9.

Brade, T., Gessert, S., Kühl, M., Pandur, P., 2007. The amphibian second heart field: Xenopus islet-1 is required for cardiovascular development. Dev. Biol. https://doi.org/10.1016/j.ydbio.2007.08.004.

Bradley, L.C., Snape, A., Bhatt, S., Wilkinson, D.G., 1993. The structure and expression of the *Xenopus* Krox-20 gene: conserved and divergent patterns of expression in rhombomeres and neural crest. Mech. Dev. 40, 73–84. https://doi.org/10.1016/0925-4773(93)90089-G.

Bugner, V., Tecza, A., Gessert, S., Kühl, M., 2011. Peter Pan functions independently of its role in ribosome biogenesis during early eye and craniofacial cartilage development in Xenopus laevis. Development 138, 2369–2378. https://doi.org/10.1242/dev.060160.

Bundesamt für Verbraucherschutz und Lebensmittelsicherheit, 2022. Zulassungen für Notfallsituationen.https://www.bvl.bund.de/DE/Arbeitsbereiche/04_Pflanzenschutzmittel/01_Aufgaben/02_ZulassungPSM/01_ZugelPSM/02_Notfallzulassungen/psm_ZugelPSM_notfallzulassungen_node.html#doc11031262bodyText7 (last accessed 27.09.2023).

Çamlıca, Y., Bediz, S.C., Çömelekoğlu, Ü., Yilmaz, Ş.N., 2019. Toxic effect of acetamiprid on Rana ridibunda sciatic nerve (electrophysiological and histopathological potential). Drug Chem. Toxicol. 42, 264–269. https://doi.org/10.1080/01480545.2018.1442475.

Cavanaugh, A.M., Huang, J., Chen, J.-N., 2015. Two developmentally distinct populations of neural crest cells contribute to the zebrafish heart. Dev. Biol. 404, 103–112. https://doi.org/10.1016/j.ydbio.2015.06.002.

Cerrizuela, S., Vega-Lopez, G.A., Aybar, M.J., 2020. The role of teratogens in neural crest development. Birth Defects Research 112, 584–632. https://doi.org/10.1002/bdr2.1644.

Chrétien, F., Giroux, I., Thériault, G., Gagnon, P., Corriveau, J., 2017. Surface runoff and subsurface tile drain losses of neonicotinoids and companion herbicides at edge-of-field. Environ. Pollut. 224, 255–264. https://doi.org/10.1016/j.envpol.2017.02.002.

Cizelsky, W., Hempel, A., Metzig, M., Tao, S., Hollemann, T., Kühl, M., Kühl, S.J., 2013. Sox4 And sox11 Function during Xenopus laevis Eye Development. PLoS One. https://doi.org/10.1371/journal.pone.0069372.

Collins, J., 2010. Amphibian decline and extinction: What we know and what we need to learn. Dis. Aquat. Org. 92, 93–99. https://doi.org/10.3354/dao02307.

European Commission, 2018. Commission Implementing Regulation (EU) 2018/784 of 29 May 2018 amending Implementing Regulation (EU) No 540/2011 as regards the conditions of approval of the active substance clothianidin. Official Journal of the European Union. https://eur-lex.europa.eu/legal-content/EN/TXT/PDF/?uri=CELEX:32018R0784 (last accessed: 27.09.2023).

Crane, J.F., Trainor, P.A., 2006. Neural Crest Stem and Progenitor Cells. Annu. Rev. Cell Dev. Biol. 22, 267–286. https://doi.org/10.1146/annurev.cellbio.22.010305.103814.

Danis, B.E.G., Marlatt, V.L., 2021. Investigating Acute and Subchronic Effects of Neonicotinoids on Northwestern Salamander Larvae. Arch Environ Contam Toxicol 80, 691–707. https://doi.org/10.1007/s00244-021-00840-4.

Dennery, P.A., 2007. Effects of oxidative stress on embryonic development. Birth Defects Research Pt C 81, 155–162. https://doi.org/10.1002/bdrc.20098.

Douglas, M.R., Tooker, J.F., 2015. Large-Scale Deployment of Seed Treatments Has Driven Rapid Increase in Use of Neonicotinoid Insecticides and Preemptive Pest Management in U.S. Field Crops. Environ. Sci. Technol. 49, 5088–5097. https://doi.org/10.1021/es506141g.

FAO. 2023. World Food and Agriculture – Statistical Yearbook 2023. Rome. https://doi.org/10.4060/cc8166en.

Faro, L.R.F., Tak-Kim, H., Alfonso, M., Durán, R., 2019. Clothianidin, a neonicotinoid insecticide, activates α4β2, α7 and muscarinic receptors to induce in vivo dopamine release from rat striatum. Toxicology 426, 152285. https://doi.org/10.1016/j.tox.2019.152285.

Environmental Fate and Effects Division Office of Pesticide Programs, 2023. Imidacloprid, Thiamethoxam and Clothianidin: Draft Predictions of Likelihood of Jeopardy and Adverse Modification for Federally Listed Endangered and Threatened Species and Designated Critical Habitats. https://www.epa.gov/system/files/documents/2023-05/ESA-JAM-Analysis.pdf (last accessed: 27.09.2023).

Finnegan, M.C., Baxter, L.R., Maul, J.D., Hanson, M.L., Hoekstra, P.F., 2017. Comprehensive characterization of the acute and chronic toxicity of the neonicotinoid insecticide thiamethoxam to a suite of aquatic primary producers, invertebrates, and fish: Thiamethoxam acute and chronic aquatic toxicity. Environ Toxicol Chem 36, 2838–2848. https://doi.org/10.1002/etc.3846.

Flach, H., Krieg, J., Hoffmeister, M., Dietmann, P., Reusch, A., Wischmann, L., Kernl, B., Riegger, R., Oess, S., Kühl, S.J., 2018. Nosip functions during vertebrate eye and cranial cartilage development. Dev. Dyn. https://doi.org/10.1002/dvdy.24659.

Flach, H., Basten, T., Schreiner, C., Dietmann, P., Greco, S., Nies, L., Roßmanith, N., Walter, S., Kühl, M., Kühl, S.J., 2021. Retinol binding protein 1 affects Xenopus anterior neural development via all-trans retinoic acid signaling. Dev. Dyn. 250, 1096–1112. https://doi.org/10.1002/dvdy.313.

Flach, H., Lenz, A., Pfeffer, S., Kühl, M., Kühl, S.J., 2022. Impact of glyphosate-based herbicide on early embryonic development of the amphibian *Xenopus laevis*. Aquat. Toxicol. 244, 106081 https://doi.org/10.1016/j.aquatox.2022.106081.

Flach, H., Dietmann, P., Liess, M., Kühl, M., Kühl, S.J., 2023a. Glyphosate without Co-formulants affects embryonic development of the south african clawed frog *Xenopus laevis*. Ecotoxicol. Environ. Saf. 260, 115080 https://doi.org/10.1016/j.ecoenv.2023.115080.

Flach, H., Geiß, K., Lohse, K.-A., Feickert, M., Dietmann, P., Pfeffer, S., Kühl, M., Kühl, S. J., 2023b. The neonicotinoid thiacloprid leads to multiple defects during early embryogenesis of the South African clawed frog (Xenopus laevis). Food Chem. Toxicol. 176, 113761 https://doi.org/10.1016/j.fct.2023.113761.

Foley, J.A., DeFries, R., Asner, G.P., Barford, C., Bonan, G., Carpenter, S.R., Chapin, F.S., Coe, M.T., Daily, G.C., Gibbs, H.K., Helkowski, J.H., Holloway, T., Howard, E.A., Kucharik, C.J., Monfreda, C., Patz, J.A., Prentice, I.C., Ramankutty, N., Snyder, P.K., 2005. Global Consequences of Land Use. Science 309, 570–574. https://doi.org/10.1126/science.1111772.

Ford, K.A., Casida, J.E., 2006. Unique and Common Metabolites of Thiamethoxam, Clothianidin, and Dinotefuran in Mice. Chem. Res. Toxicol. 19, 1549–1556. https://doi.org/10.1021/tx0601859.

Furukawa, T., Kozak, C.A., Cepko, C.L., 1997. rax, a novel paired-type homeobox gene, shows expression in the anterior neural fold and developing retina. PNAS 94, 3088–3093. https://doi.org/10.1073/pnas.94.7.3088.

Gao, L., Li, S., Zhang, J., Liang, C., Chen, E., Zhang, S., Chuai, M., Bao, Y., Wang, G., Yang, X., 2016. Excess imidacloprid exposure causes the heart tube malformation of

chick embryos. J. Agric. Food Chem. 64, 9078–9088. https://doi.org/10.1021/acs.jafc.6b03381.
Garriock, R.J., Meadows, S.M., Krieg, P.A., 2005. Developmental expression and comparative genomic analysis of *Xenopus* cardiac myosin heavy chain genes. Dev. Dyn. 233, 1287–1293. https://doi.org/10.1002/dvdy.20460.
Gentsch, G.E., Spruce, T., Monteiro, R.S., Owens, N.D.L., Martin, S.R., Smith, J.C., 2018. Innate Immune Response and Off-Target Mis-splicing Are Common Morpholino-Induced Side Effects in Xenopus. Dev. Cell 44 (5), 597–610.e10. https://doi.org/10.1016/j.devcel.2018.01.022.
Gerber, W.V., Vokes, S.A., Zearfoss, N.R., Krieg, P.A., 2002. A role for the rna-binding protein, hermes, in the regulation of heart development. Dev. Biol. 247, 116–126. https://doi.org/10.1006/dbio.2002.0678.
Gessert, S., Kühl, M., 2009. Comparative gene expression analysis and fate mapping studies suggest an early segregation of cardiogenic lineages in *Xenopus laevis*. Dev. Biol. 334, 395–408. https://doi.org/10.1016/j.ydbio.2009.07.037.
Gessert, S., Maurus, D., Rössner, A., Kühl, M., 2007. Pescadillo is required for *Xenopus laevis* eye development and neural crest migration. Dev. Biol. https://doi.org/10.1016/j.ydbio.2007.07.037.
Gessert, S., Maurus, D., Brade, T., Walther, P., Pandur, P., Kühl, M., 2008. DM-GRASP/ALCAM/CD166 is required for cardiac morphogenesis and maintenance of cardiac identity in first heart field derived cells. Dev. Biol. https://doi.org/10.1016/j.ydbio.2008.06.013.
Gessert, S., Bugner, V., Tecza, A., Pinker, M., Kühl, M., 2010. FMR1/FXR1 and the miRNA pathway are required for eye and neural crest development. Dev. Biol. https://doi.org/10.1016/j.ydbio.2010.02.031.
Girolami, V., Mazzon, L., Squartini, A., Mori, N., Marzaro, M., Di Bernardo, A., Greatti, M., Giorio, C., Tapparo, A., 2009. Translocation of Neonicotinoid Insecticides From Coated Seeds to Seedling Guttation Drops: A Novel Way of Intoxication for Bees. ec 102, 1808–1815. https://doi.org/10.1603/029.102.0511.
Granados-Riveron, J.T., Ghosh, T.K., Pope, M., Bu'Lock, F., Thornborough, C., Eason, J., Kirk, E.P., Fatkin, D., Feneley, M.P., Harvey, R.P., Armour, J.A.L., Brook, J.D., 2010. α-Cardiac myosin heavy chain (MYH6) mutations affecting myofibril formation are associated with congenital heart defects. Hum. Mol. Genet. https://doi.org/10.1093/hmg/ddq315.
Guo, Y., Dorn, T., Kühl, S.J., Linnemann, A., Rothe, M., Pfister, A.S., Vainio, S., Laugwitz, K.-L., Moretti, A., Kühl, M., 2019. The Wnt inhibitor Dkk1 is required for maintaining the normal cardiac differentiation program in Xenopus laevis. Dev. Biol. 449, 1–13. https://doi.org/10.1016/j.ydbio.2019.02.009.
Győri, J., Farkas, A., Stolyar, O., Székács, A., Mörtl, M., Vehovszky, Á., 2017. Inhibitory effects of four neonicotinoid active ingredients on acetylcholine esterase activity. Acta Biol Hung. 68 (4), 345–357. https://doi.org/10.1556/018.68.2017.4.1. PMID: 29262703.
Hayasaka, D., Korenaga, T., Sánchez-Bayo, F., Goka, K., 2012. Differences in ecological impacts of systemic insecticides with different physicochemical properties on biocenosis of experimental paddy fields. Ecotoxicology 21, 191–201. https://doi.org/10.1007/s10646-011-0778-y.
Hemmati-Brivanlou, A., Frank, D., Bolce, M.E., Brown, B.D., Sive, H.L., Harland, R.M., 1990. Localization of specific mRNAs in *Xenopus* embryos by whole-mount in situ hybridization. Development.
Hempel, A., Kühl, S.J., Rothe, M., Rao Tata, P., Sirbu, I.O., Vainio, S.J., Kühl, M., 2017. The CapZ interacting protein Rcsd1 is required for cardiogenesis downstream of Wnt11a in Xenopus laevis. Dev. Biol. 424, 28–39. https://doi.org/10.1016/j.ydbio.2017.02.014.
Hollemann, T., Bellefroid, E., Pieler, T., 1998. The *Xenopus* homologue of the *Drosophila* gene tailless has a function in early eye development. Development 125, 2425–2432.
Hopwood, N.D., Pluck, A., Gurdon, J.B., 1989. A *Xenopus* mRNA related to *Drosophila* twist is expressed in response to induction in the mesoderm and the neural crest. Cell 59, 893–903. https://doi.org/10.1016/0092-8674(89)90612-0.
Huyen, V.N., Van Song, N., Thuy, N.T., Dung, L.T.P., Hoan, L.K., 2020. Effects of pesticides on farmers' health in Tu Ky district, Hai Duong province. Vietnam. Sustainable Futures 2, 100026. https://doi.org/10.1016/j.sftr.2020.100026.
Ihara, M., Matsuda, K., 2018. Neonicotinoids: molecular mechanisms of action, insights into resistance and impact on pollinators. Curr. Opin. Insect Sci. 30, 86–92. https://doi.org/10.1016/j.cois.2018.09.009.
Ikenaka, Y., Miyabara, Y., Ichise, T., Nakayama, S., Nimako, C., Ishizuka, M., Tohyama, C., 2019. Exposures of children to neonicotinoids in pine wilt disease control areas. Enviro Toxic and Chemistry 38, 71–79. https://doi.org/10.1002/etc.4316.
Jemec, A., Tišler, T., Drobne, D., Sepčić, K., Fournier, D., Trebše, P., 2007. Comparative toxicity of imidacloprid, of its commercial liquid formulation and of diazinon to a non-target arthropod, the microcrustacean *Daphnia magna*. Chemosphere 68, 1408–1418. https://doi.org/10.1016/j.chemosphere.2007.04.015.
Jenkins, J.A., Hartop, K.R., Bukhari, G., Howton, D.E., Smalling, K.L., Mize, S.V., Hladik, M.L., Johnson, D., Draugelis-Dale, R.O., Brown, B.L., 2021. Juvenile African Clawed Frogs (Xenopus laevis) Express Growth, Metamorphosis, Mortality, Gene Expression, and Metabolic Changes When Exposed to Thiamethoxam and Clothianidin. IJMS 22, 13291. https://doi.org/10.3390/ijms222413291.
Jeschke, P., Nauen, R., Schindler, M., Elbert, A., 2011. Overview of the status and global strategy for neonicotinoids. J. Agric. Food Chem. 59, 2897–2908. https://doi.org/10.1021/jf101303g.
Kagabu, S., 2011. Discovery of imidacloprid and further developments from strategic molecular designs. J. Agric. Food Chem. 59, 2887–2896. https://doi.org/10.1021/jf101824y.
Karmakar, R., Singh, S.B., Kulshrestha, G., 2009. Kinetics and mechanism of the hydrolysis of thiamethoxam. J. Environ. Sci. Health B 44, 435–441. https://doi.org/10.1080/03601230902934785.
Kerner, M., Flach, H., Dietmann, P., Kühl, M., Kühl, S.J., 2023. The impact of the insecticide acetamiprid on the embryogenesis of the aquatic model organism *Xenopus laevis*. Environ. Toxicol. Pharmacol. 103, 104278 https://doi.org/10.1016/j.etap.2023.104278.
Kiem, L.M., Dietmann, P., Linnemann, A., Schmeisser, M.J., Kühl, S.J., 2017. The Nedd4 binding protein 3 is required for anterior neural development in Xenopus laevis. Dev. Biol. https://doi.org/10.1016/j.ydbio.2017.01.009.
Le Douarin, N.M., Brito, J.M., Creuzet, S., 2007. Role of the neural crest in face and brain development. Brain Res. Rev. 55, 237–247. https://doi.org/10.1016/j.brainresrev.2007.06.023.
Lechenet, M., Dessaint, F., Py, G., Makowski, D., Munier-Jolain, N., 2017. Reducing pesticide use while preserving crop productivity and profitability on arable farms. Nat. Plants 3, 17008. https://doi.org/10.1038/nplants.2017.8.
Lee, V.M., Sechrist, J.W., Luetolf, S., Bronner-Fraser, M., 2003. Both neural crest and placode contribute to the ciliary ganglion and oculomotor nerve. Dev. Biol. 263, 176–190. https://doi.org/10.1016/j.ydbio.2003.07.004.
Liu, M., Wang, G., Zhang, S.-Y., Zhong, S., Qi, G.-L., Wang, C.-J., Chuai, M., Lee, K.K.H., Lu, D.-X., Yang, X., 2016. From the Cover: Exposing Imidacloprid Interferes With Neurogenesis Through Impacting on Chick Neural Tube Cell Survival. Toxicol. Sci. 153, 137–148. https://doi.org/10.1093/toxsci/kfw111.
Liu, X., Zhang, Q., Li, S., Mi, P., Chen, D., Zhao, X., Feng, X., 2018. Developmental toxicity and neurotoxicity of synthetic organic insecticides in zebrafish (Danio rerio): A comparative study of deltamethrin, acephate, and thiamethoxam. Chemosphere 199, 16–25. https://doi.org/10.1016/j.chemosphere.2018.01.176.
Lu, Z., Challis, J.K., Wong, C.S., 2015. Quantum Yields for Direct Photolysis of Neonicotinoid Insecticides in Water: Implications for Exposure to Nontarget Aquatic Organisms. Environ. Sci. Technol. Lett. 2, 188–192. https://doi.org/10.1021/acs.estlett.5b00136.
Lupo, G., Andreazzoli, M., Gestri, G., Liu, Y., He, R.-Q., Barsacchi, G., 2000. Homeobox genes in the genetic control of eye development. Int. J. Dev. Biol. 44 (6), 627–636.
Ma, X., Li, H., Xiong, J., Mehler, W.T., You, J., 2019. Developmental Toxicity of a Neonicotinoid Insecticide, Acetamiprid to Zebrafish Embryos. J. Agric. Food Chem. 67, 2429–2436. https://doi.org/10.1021/acs.jafc.8b05373.
Mahai, G., Wan, Y., Xia, W., Wang, A., Qian, X., Li, Y., He, Z., Li, Y., Xu, S., 2022. Exposure assessment of neonicotinoid insecticides and their metabolites in Chinese women during pregnancy: A longitudinal study. Sci Total Environ. 818, 151806 https://doi.org/10.1016/j.scitotenv.2021.151806. Epub 2021 Nov 20 PMID: 34808166.
Malev, O., Klobučar, R.S., Fabbretti, E., Trebše, P., 2012. Comparative toxicity of imidacloprid and its transformation product 6-chloronicotinic acid to non-target aquatic organisms: Microalgae *Desmodesmus subspicatus* and amphipod *Gammarus fossarum*. Pestic. Biochem. Physiol. 104, 178–186. https://doi.org/10.1016/j.pestbp.2012.07.008.
Malhotra, N., Chen, K.-H.-C., Huang, J.-C., Lai, H.-T., Uapipatanakul, B., Roldan, M.J.M., Macabeo, A.P.G., Ger, T.-R., Hsiao, C.-D., 2021. Physiological Effects of Neonicotinoid Insecticides on Non-Target Aquatic Animals—An Updated Review. IJMS 22, 9591. https://doi.org/10.3390/ijms22179591.
Marlatt, V.L., Leung, T.Y.G., Calbick, S., Metcalfe, C., Kennedy, C., 2019. Sub-lethal effects of a neonicotinoid, clothianidin, on wild early life stage sockeye salmon (Oncorhynchus nerka). Aquat. Toxicol. 217, 105335 https://doi.org/10.1016/j.aquatox.2019.105335.
Matsuda, K., Buckingham, S.D., Kleier, D., Rauh, J.J., Grauso, M., Sattelle, D.B., 2001. Neonicotinoids: insecticides acting on insect nicotinic acetylcholine receptors. Trends Pharmacol. Sci. 22, 573–580. https://doi.org/10.1016/S0165-6147(00)01820-4.
Megchún-García, J.V., Chávez, M.D.R.C., Rodríguez-Lagunes, D.A., Adame-García, J., Murguía-González, J., Lango- Reynoso, F., Leyva-Ovalle, O.R., 2018. Use of thiamethoxam, associated with insect populations in Papaya (Carica Papaya Linnaeus) cultivation. Int. J. Res. Granthaalayah 6, 428–439. https://doi.org/10.29121/granthaalayah.v6.i1.2018.1650.
Miles, J.C., Hua, J., Sepulveda, M.S., Krupke, C.H., Hoverman, J.T., 2017. Effects of clothianidin on aquatic communities: Evaluating the impacts of lethal and sublethal exposure to neonicotinoids. PLoS One 12, 1–24. https://doi.org/10.1371/journal.pone.0174171.
Muranishi, Y., Terada, K., Furukawa, T., 2012. An essential role for Rax in retina and neuroendocrine system development. Dev Growth Differ 54, 341–348. https://doi.org/10.1111/j.1440-169X.2012.01337.x.
Nieuwkoop, P.D., Faber, J., 1954. Normal Table of Xenopus laevis (Daudin): A Systematical and Chronological Survey of the Development from the Fertilized Egg till the End of Metamorphosis. North-Holland Pub. Co., Amsterdam.
Ortiz-Santaliestra, M.E., Marco, A., Fernández, M.J., Lizana, M., 2006. Influence of developmental stage on sensitivity to ammonium nitrate of aquatic stages of amphibians. Environ. Toxicol. Chem. 25, 105–111. https://doi.org/10.1897/05-023r.1.
Osterauer, R., Köhler, H.R., 2008. Temperature-dependent effects of the pesticides thiacloprid and diazinon on the embryonic development of zebrafish (Danio rerio). Aquat. Toxicol. 86, 485–494. https://doi.org/10.1016/j.aquatox.2007.12.013.
Park, B.-Y., Saint-Jeannet, J.-P., 2008. Hindbrain-derived Wnt and Fgf signals cooperate to specify the otic placode in Xenopus. Dev. Biol. 324, 108–121. https://doi.org/10.1016/j.ydbio.2008.09.009.
Peterkin, T., Gibson, A., Patient, R., 2007. Redundancy and evolution of GATA factor requirements in development of the myocardium. Dev. Biol. 311, 623–635. https://doi.org/10.1016/j.ydbio.2007.08.018.
Qi, S., Wang, D., Zhu, L., Teng, M., Wang, C., Xue, X., Wu, L., 2018. Neonicotinoid insecticides imidacloprid, guadipyr, and cycloxaprid induce acute oxidative stress in

Daphnia magna. Ecotoxicol Environ Saf. 148, 352–358. https://doi.org/10.1016/j.ecoenv.2017.10.042. Epub 2017 Nov 6 PMID: 29096261.

Radwan, M.A., Mohamed, M.S., 2013. Imidacloprid induced alterations in enzyme activities and energy reserves of the land snail, *Helix aspersa*. Ecotoxicol. Environ. Saf. 95, 91–97. https://doi.org/10.1016/j.ecoenv.2013.05.019.

Robinson, S.A., Richardson, S.D., Dalton, R.L., Maisonneuve, F., Bartlett, A.J., De Solla, S. R., Trudeau, V.L., Waltho, N., 2019. Assessment of Sublethal Effects of Neonicotinoid Insecticides on the Life-History Traits of 2 Frog Species. Enviro Toxic and Chemistry 38, 1967–1977. https://doi.org/10.1002/etc.4511.

Roessink, I., Merga, L.B., Zweers, H.J., Van Den Brink, P.J., 2013. the neonicotinoid imidacloprid shows high chronic toxicity to mayfly nymphs. Environ. Toxicol. Chem. 32, 1096–1100. https://doi.org/10.1002/etc.2201.

Rothe, M., Kanwal, N., Dietmann, P., Seigfried, F.A., Hempel, A., Schütz, D., Reim, D., Engels, R., Linnemann, A., Schmeisser, M.J., Bockmann, J., Kühl, M., Boeckers, T.M., Kühl, S.J., 2017. An Epha4/Sipa1l3/Wnt pathway regulates eye development and lens maturation. Development (Cambridge). https://doi.org/10.1242/dev.147462.

Sánchez-Bayo, F., Goka, K., 2005. Unexpected effects of zinc pyrithione and imidacloprid on Japanese medaka fish (Oryzias latipes). Aquat. Toxicol. 74, 285–293. https://doi.org/10.1016/j.aquatox.2005.06.003.

Saumweber, E., Mzoughi, S., Khadra, A., Werberger, A., Schumann, S., Guccione, E., Schmeisser, M.J., Kühl, S.J., 2024. Prdm15 acts upstream of Wnt4 signaling in anterior neural development of Xenopus laevis. Front. Cell Dev. Biol. https://doi.org/10.3389/fcell.2024.1316048.

Schäfer, B., 2008. Die Neonicotinoide. Nicotin und die Neonicotinoide – Teil 2. Chemie in Nserer Zeit 42, 408–424. https://doi.org/10.1002/ciuz.200800465.

Schindelin, J., Arganda-Carreras, I., Frise, E., Kaynig, V., Longair, M., Pietzsch, T., Preibisch, S., Rueden, C., Saalfeld, S., Schmid, B., Tinevez, J.-Y., White, D.J., Hartenstein, V., Eliceiri, K., Tomancak, P., Cardona, A., 2012. Fiji: an open-source platform for biological-image analysis. Nat Methods 9, 676–682. https://doi.org/10.1038/nmeth.2019.

Schlosser, G., 2006. Induction and specification of cranial placodes. Dev. Biol. 294, 303–351. https://doi.org/10.1016/j.ydbio.2006.03.009.

Schlosser, G., Ahrens, K., 2004. Molecular anatomy of placode development in *Xenopus laevis*. Dev. Biol. 271, 439–466. https://doi.org/10.1016/j.ydbio.2004.04.013.

Schlosser, G., Northcutt, R.G., 2000. Development of neurogenic placodes in *Xenopus laevis*. J. Comp. Neurol. 418 (2), 121–146. PMID: 10701439.

Schuff, M., Rössner, A., Wacker, S.A., Donow, C., Gessert, S., Knöchel, W., 2007. FoxN3 is required for craniofacial and eye development of *Xenopus laevis*. Dev. Dyn. https://doi.org/10.1002/dvdy.21007.

Seigfried, F.A., Cizelsky, W., Pfister, A.S., Dietmann, P., Walther, P., Kühl, M., Kühl, S.J., 2017. Frizzled 3 acts upstream of Alcam during embryonic eye development. Dev. Biol. https://doi.org/10.1016/j.ydbio.2017.04.004.

Siregar, P., Suryanto, M.E., Chen, K.-H.-C., Huang, J.-C., Chen, H.-M., Kurnia, K.A., Santoso, F., Hussain, A., Ngoc Hieu, B.T., Saputra, F., Audira, G., Roldan, M.J.M., Fernandez, R.A., Macabeo, A.P.G., Lai, H.-T., Hsiao, C.-D., 2021. Exploiting the Freshwater Shrimp *Neocaridina denticulata* as Aquatic Invertebrate Model to Evaluate Nontargeted Pesticide Induced Toxicity by Investigating Physiologic and Biochemical Parameters. Antioxidants 10, 391. https://doi.org/10.3390/antiox10030391.

Sive, H.L., Grainger, R.M., Harland, R.M., 2000. Early Development of *Xenopus Laevis*: A Laboratory Manual. Cold Spring Harbor Laboratory Press, N.Y.

Strate, I., Min, T.H., Iliev, D., Pera, E.M., 2009. Retinol dehydrogenase 10 is a feedback regulator of retinoic acid signalling during axis formation and patterning of the central nervous system. Development 136, 461–472. https://doi.org/10.1242/dev.024901.

Tamanoue, Y., Hongo, I., Okamoto, H., 2006. Involvement of a Xenopus nuclear GTP-binding protein in optic primordia formation. Dev Growth Differ 48, 575–585. https://doi.org/10.1111/j.1440-169X.2006.00891.x.

Tandon, P., Conlon, F., Furlow, J.D., Horb, M.E., 2017. Expanding the genetic toolkit in *Xenopus*: Approaches and opportunities for human disease modeling. Dev. Biol. 426, 325–335. https://doi.org/10.1016/j.ydbio.2016.04.009.

Tišler, T., Jemec, A., Mozetič, B., Trebše, P., 2009. Hazard identification of imidacloprid to aquatic environment. Chemosphere 76, 907–914. https://doi.org/10.1016/j.chemosphere.2009.05.002.

Todey, S.A., Fallon, A.M., Arnold, W.A., 2018. Neonicotinoid insecticide hydrolysis and photolysis: Rates and residual toxicity. Enviro Toxic and Chemistry 37, 2797–2809. https://doi.org/10.1002/etc.4256.

Tomizawa, M., Casida, J.E., 2003. Selective Toxicity of Neonicotinoids Attributable to Specificity of Insect and Mammalian Nicotinic Receptors. Annu. Rev. Entomol. 48, 339–364. https://doi.org/10.1146/annurev.ento.48.091801.112731.

Van Dijk, T.C., Van Staalduinen, M.A., Van Der Sluijs, J.P., 2013. Macro-Invertebrate Decline in Surface Water Polluted with Imidacloprid. PLoS One 8, e62374.

Vega-Lopez, G.A., Cerrizuela, S., Tribulo, C., Aybar, M.J., 2018. Neurocristopathies: New insights 150 years after the neural crest discovery. Dev. Biol. 444, S110–S143. https://doi.org/10.1016/j.ydbio.2018.05.013.

Wan, Y., Han, Q., Wang, Y., He, Z., 2020. Five degradates of imidacloprid in source water, treated water, and tap water in Wuhan, central China. Sci. Total Environ. 741, 140227 https://doi.org/10.1016/j.scitotenv.2020.140227.

Wang, H., Wang, C., Long, Q., Zhang, Y., Wang, M., Liu, J., Qi, X., Cai, D., Lu, G., Sun, J., Yao, Y.-G., Chan, Wood Yee, Chan, Wai Yee, Deng, Y., Zhao, H., 2021. Kindlin2 regulates neural crest specification via integrin-independent regulation of the FGF signaling pathway.

Wang, C.J., Wang, G., Wang, X.Y., Liu, M., Chuai, M., Lee, K.K.H., He, X.S., Lu, D.X., Yang, X., 2016. Imidacloprid Exposure Suppresses Neural Crest Cells Generation during Early Chick Embryo Development. J. Agric. Food Chem. 64, 4705–4715. https://doi.org/10.1021/acs.jafc.6b01478.

Williams, A.L., Bohnsack, B.L., 2015. Neural crest derivatives in ocular development: Discerning the eye of the storm. Birth Defects Research Pt C 105, 87–95. https://doi.org/10.1002/bdrc.21095.

Wu, S., Li, X., Liu, X., Yang, G., An, X., Wang, Q., Wang, Y., 2018. Joint toxic effects of triazophos and imidacloprid on zebrafish (Danio rerio). Environ. Pollut. 235, 470–481. https://doi.org/10.1016/j.envpol.2017.12.120.

YongFan, P., 2015. Progress in pesticide risk assessment and phasing-out of highly hazardous pesticides in Asia., RAP Publication (FAO). Food & Agriculture Org. https://books.google.de/books?id=BEttDwAAQBAJ.

Zheng, W., Liu, W., 1999. Kinetics and mechanism of the hydrolysis of imidacloprid. Pestic. Sci. 55, 482–485. https://doi.org/10.1002/(SICI)1096-9063(199904)55:4<482::AID-PS932>3.0.CO;2-3.

Zhong, K., Meng, Y., Wu, J., Wei, Y., Huang, Y., Ma, J., Lu, H., 2021. Effect of flupyradifurone on zebrafish embryonic development. Environ. Pollut. 285, 117323 https://doi.org/10.1016/j.envpol.2021.117323.

Ziman, M.R., Rodger, J., Chen, P., Papadimitriou, J.M., Dunlop, S.A., Beazley, L.D., 2001. Pax genes in development and maturation of the vertebrate visual system: Implications for optic nerve regeneration. Histol. Histopathol. 239–249. https://doi.org/10.14670/HH-16.239.